

B



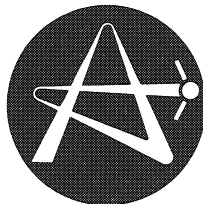
29 OCT. 1984

AECL 8440

9

AECL-8440

ATOMIC ENERGY
OF CANADA LIMITED



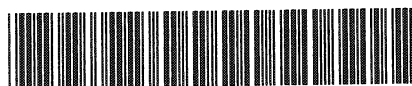
L'ÉNERGIE ATOMIQUE
DU CANADA LIMITÉE

**DETAILS OF THE GENERAL NUMERICAL SOLUTIONS OF
THE FRIEDBERG-LEE SOLITON MODEL FOR
GROUND AND EXCITED STATES**

**Détails des solutions numériques générales
du modèle Soliton de Friedberg-Lee pour
les états fondamentaux et excités**

Th. KÖPPEL and M. HARVEY

CERN LIBRARIES, GENEVA



CM-P00067679

Chalk River Nuclear Laboratories

Laboratoires nucléaires de Chalk River

Chalk River, Ontario

June 1984 juin

**DETAILS OF THE GENERAL NUMERICAL SOLUTIONS OF THE FRIEDBERG-LEE
SOLITON MODEL FOR GROUND AND EXCITED STATES**

Th. Köppel and M. Harvey

**Theoretical Physics Branch
Chalk River Nuclear Laboratories,
Chalk River, Ontario, Canada K0J 1J0
1984 June**

AECL-8440

L'ENERGIE ATOMIQUE DU CANADA, LIMITEE

Détails des solutions numériques générales
du modèle Soliton de Friedberg-Lee
pour les états fondamentaux et excités

par

Th. Köppel† et M. Harvey

Résumé

Une nouvelle méthode numérique est employée pour résoudre les équations de mouvement du modèle Soliton de Friedberg-Lee pour les états fondamentaux et les états excités sphériquement symétriques. Des résultats généraux ont été obtenus dans une vaste gamme de paramètres. Les constantes de couplage critiques et les nombres de particules critiques ont été déterminés au-dessous desquels les solutions du Soliton cessent d'exister. Les propriétés statiques du proton semblent montrer que dans sa formulation actuelle le modèle ne parvient pas à accommoder toutes les données expérimentales de n'importe quel ensemble de paramètres.

Département de physique théorique
Laboratoires nucléaires de Chalk River
Chalk River, Ontario, Canada K0J 1J0

Juin 1984

AECL-8440

DETAILS OF THE GENERAL NUMERICAL SOLUTIONS OF THE FRIEDBERG-LEE
SOLITON MODEL FOR GROUND AND EXCITED STATES

Th. Köppel[†] and M. Harvey

Abstract

A new numerical method is applied to solving the equations of motion of the Friedberg-Lee Soliton model for both ground and spherically symmetric excited states. General results have been obtained over a wide range of parameters. Critical coupling constants and critical particle numbers have been determined below which soliton solutions cease to exist. The static properties of the proton are considered to show that as presently formulated the model fails to fit all experimental data for any set of parameters.

[†] Natural Sciences & Engineering Research Council of Canada
Post-Doctoral Fellow

Theoretical Physics Branch
Chalk River Nuclear Laboratories,
Chalk River, Ontario, Canada K0J 1J0
1984 June

AECL-8440

I. Introduction

Soliton models have been proposed as the effective manifestation of confinement in QCD¹⁻¹⁴. In these models the confinement of quarks is realized through their interaction with a scalar soliton field (σ -field). In the particular model of Friedberg & Lee⁸⁻¹¹, the soliton solution of a mean scalar σ -field is made possible through introduction of a non-linear self energy potential $U(\sigma)$. The states $(\psi_k(\vec{r}))$ of the quarks and σ -fields then satisfy, in the mean-field approximation, the coupled set of equations

$$[-i\vec{\alpha}\vec{\nabla} + \beta m + \beta g \sigma(\vec{r})] \psi_k(\vec{r}) = \epsilon_k \psi_k(\vec{r}) \quad (1.1a)$$

$$-\nabla^2 \sigma(\vec{r}) + \frac{\partial U(\sigma)}{\partial \sigma} = -g \sum_{k \text{ occ.}} \bar{\psi}_k(\vec{r}) \psi_k(\vec{r}) \quad (1.1b)$$

with

$$\int \psi_k^\dagger(\vec{r}) \psi_k(\vec{r}) d^3 r = 1 \quad (1.1c)$$

where $\vec{\alpha}$ and β are the conventional Dirac matrices. Here the quarks are coupled to the σ -field by a coupling constant g .

An analysis of the solutions resulting from the set of Eqs. (1.1a to c) has been given by Friedberg & Lee⁹. They show that solutions can take on the characteristics of either the MIT¹⁵ or the SLAC¹⁶ bag model, depending on the choice of parameters in $U(\sigma)$. They also show numerical solutions for a particular choice of parameters whereby the coupled Eqs. (1.1a and b) reduce to two coupled, first-order differential equations which are parameter free: the parameters in this case having been absorbed in the scaling. Numerical solutions of the set of Eqs. (1.1a to c) have been given for selected choice of parameters by Goldflam & Willets¹² and later by Saly & Sundaresan¹³. The approach adopted by these authors in solving the coupled set of Eqs. (1.1) is an iterative one whereby first a guess is made for the σ -field and the solution of the Dirac eigenvalue-problem in Eq. (1.1a) found numerically. With this choice of the Dirac-functions in the source term, Eq. (1.1b) is solved numerically for a new

estimate of the σ mean field. This process is iterated to convergence - if possible.

The main purpose of this paper is to show how the set of coupled differential Eqs. (1.1a to c) can be solved simultaneously. The method we adopt immediately illustrates many of the general features deduced by Friedberg and Lee as well as uncovering other interesting scaling properties of the solutions. It is immediately obvious from our results when soliton solutions should exist, i.e. why the iterative procedure failed at times. Results of the model have been obtained with parameters varying over many decades. General results have also been found for quarks excited to higher quantum states.

The structure of the paper is as follows. In Section II we review features of the soliton model and then, in Section III, discuss the application of the model to a spherically symmetric ground state. Here we show a useful scaling which allows the equations of motion to be treated as a boundary value problem of a set of coupled differential equations. Section IV outlines the collocation method¹⁷⁻¹⁹ which has been applied for the numerical solution of this boundary value problem. Section V shows the results of the calculations of the ground state for various parameter choices. We also consider here how close the model comes to reproducing static properties of the proton, although we believe the model must be extended before a detailed fit to hadrons is worthwhile. In Section VI we show results of application of the method to excited quark configurations. Section VII contains a summary and conclusion. A summary of the results of this report has been submitted for publication in a journal.

II. The Soliton Bag Model

The soliton bag model, as it was proposed by Friedberg & Lee⁸⁻¹¹, is given in its lowest approximation by an effective Lagrangian density

$$\mathcal{L} = \bar{\psi}(i\cancel{\partial} - m)\psi - g\bar{\psi}\sigma\psi + \frac{1}{2} \partial_{\mu}\sigma\partial^{\mu}\sigma - U(\sigma) . \quad (2.1)$$

This system consists only of the quark field ψ and the scalar gluon field σ . In this work we restrict ourselves to the above Lagrangian. We are not taking into account any counterterms, which would be used for renormalisation, and we neglect residual vector-gluon fields and Higgs fields (which would have to appear in a complete Lagrangian) and pion fields as in a chirally invariant extension of the model. The self-energy $U(\sigma)$ of the scalar field σ is parametrized in a phenomenological form (Fig. 1)

$$U(\sigma) = (\sigma - \sigma_v)^2 \{ s\sigma^2 + 2t\sigma_v\sigma + t\sigma_v^2 \} . \quad (2.2)$$

This is of quartic order in σ and has the most general form such that the minima of $U(\sigma)$ are at $\sigma=0$ and $\sigma=\alpha_v$ with $U(\alpha_v) = 0$. It is assumed that σ differs from α_v only in the presence of quark fields. Furthermore, the scalar gluon field σ is treated as a classical, time-independent c-number mean-field $\sigma(r)$, having a radial form as shown in Fig. 2. The quark field ψ can be expanded in terms of annihilation and creation operators in a complete set of quark spinor wavefunctions $\{\psi_k\}$ which satisfy the Dirac Eq. (1.1a). The scalar gluon field $\sigma(r)$ then has to satisfy the Euler-Lagrange equation of motion in Eq. (1.1b). Eqs. (1.1a) and (1.1b) represent a system of coupled differential equations, which have to be solved simultaneously with the normalization condition Eq. (1.1c). At large radius r the right-hand-side of Eq. (1.1b), the source term for the scalar σ field, drops to zero and the σ field assumes its vacuum value α_v . At small radius r , where the quark wavefunctions ψ_k are nonvanishing, the σ field has a value close to the second minimum near zero. These boundary conditions are the origin of the confinement of the quarks within the radius of the soliton bag. The total energy of this system of quarks and the soliton field is given by

$$\begin{aligned} E_{\text{tot}} &= \sum_{k_{\text{occ}}} \epsilon_k + \int \left[\frac{1}{2} (\vec{\nabla}\sigma(r))^2 + U(\sigma(r)) \right] d^3r \\ &= E_q + E_\sigma . \end{aligned} \quad (2.3)$$

III. The Ground State

The ground state of the soliton bag is the state where N quarks are in the same lowest Dirac state ψ_0 . The number of quarks would be $N=3$ for baryons and $N=2$ for mesons. The ground state s -wave Dirac spinor wavefunction ψ_0 is written as

$$\psi_0 = \begin{pmatrix} u_0(r) \\ iv_0(r) \hat{\sigma} \cdot \hat{r} \end{pmatrix} s \quad (3.1)$$

where

$$s = \begin{pmatrix} 1 \\ 0 \end{pmatrix} \quad \text{or} \quad s = \begin{pmatrix} 0 \\ 1 \end{pmatrix}.$$

The system is spherical symmetric and the Eqs. (1.1a, b and c) transform in radial coordinates to

$$\frac{du_0}{dr} = -(\epsilon_0 + m + g\sigma_0)v_0 \quad (3.2a)$$

$$\frac{dv_0}{dr} = -\frac{2}{r}v_0 + (\epsilon_0 - m - g\sigma_0)u_0 \quad (3.2b)$$

$$4\pi \int r^2 (u_0^2 + v_0^2) dr = 1 \quad (3.3)$$

$$\frac{d^2\sigma_0}{dr^2} = -\frac{2}{r} \frac{d\sigma_0}{dr} + \frac{dU(\sigma_0)}{d\sigma_0} + Ng(u_0^2 - v_0^2) \quad (3.4)$$

The solution of Eqs. (3.2) to (3.4) has to satisfy the boundary conditions

$$v_0(r=0) = 0, \quad u_0(r=\infty) = 0, \quad \sigma(r=\infty) = \sigma_v, \quad \frac{d\sigma}{dr}(r=0) = 0 \quad (3.5)$$

The bare quark mass will be taken as $m=0$. A non zero quark mass m can formally be included by shifting the soliton field σ_0 to $\sigma'_0 = \sigma_0 + \frac{m}{g}$. The soliton self-energy $U(\sigma)$ (eq. 2.2) and the boundary conditions (3.5) have to be corrected equivalently.

In the following it will be shown how the Eqs. (3.2) to (3.4), with the boundary conditions Eq. (3.5), can be transformed into a boundary value problem of a system of ordinary differential equations. In the first step, all the quantities in Eqs. (3.2) to (3.4) are scaled according to

$$\vec{r} = \frac{\vec{r}'}{g\sigma_v}, \quad \sigma = \sigma_v \sigma', \quad \varepsilon = g\sigma_v \varepsilon', \quad (3.6)$$

$$\psi_0 = \sqrt{\frac{g\sigma_v^3}{N}} \psi'_0, \quad u_0 = \sqrt{\frac{g\sigma_v^3}{N}} u'_0, \quad v_0 = \sqrt{\frac{g\sigma_v^3}{N}} v'_0$$

and the soliton self-energy $U(\sigma)$ is rewritten as

$$U(\sigma) = g^2 \sigma_v^4 U'(\sigma') \quad (3.7)$$

with

$$U'(\sigma') = (\sigma' - 1)^2 \{s' \sigma'^2 + 2t' \sigma' + t'\}$$

and

$$s = g^2 s', \quad t = g^2 t'.$$

The scaled, primed quantities are all dimensionless.

Equations (3.2) to (3.4) are rewritten in these quantities as

$$\frac{du'_0}{dr'} = -(\varepsilon'_0 + \sigma'_0) v'_0 \quad (3.8a)$$

$$\frac{dv'_0}{dr'} = -\frac{2}{r'} v'_0 + (\varepsilon'_0 - \sigma'_0) u'_0 \quad (3.8b)$$

$$4\pi \int r'^2 (u_0'^2 + v_0'^2) dr' = \eta' \quad (3.9a)$$

with

$$4\pi \int r^2 (u_0^2 + v_0^2) dr = \frac{\eta'}{Ng^2} \equiv 1 \quad (3.9b)$$

and

$$\frac{d^2 \sigma'_0}{dr'^2} = -\frac{2\sigma'_0}{r'} + \frac{dU'(\sigma'_0)}{d\sigma'_0} + (u'_0{}^2 - v'_0{}^2) \quad (3.10)$$

The boundary conditions are

$$v'_0(r'=0) = 0, \quad u'_0(r'=\infty) = 0, \quad \sigma'_0(r'=\infty) = 1, \quad \frac{d\sigma'_0}{dr'}(r'=0) = 0 \quad (3.11)$$

It is remarkable that in the set of coupled equations in Eqs. 3.8a, 3.8b and 3.10 there is no explicit dependence on the asymptotic soliton field σ_v , the coupling constant g or the particle number N . Furthermore, the main advantage achieved by the scaling of the equations is the following. The Eqs. (3.8a), (3.8b) and (3.10), together with the boundary conditions in Eq. (3.11) form a well defined boundary value problem of a system of coupled ordinary differential equations. The free parameters of this system are now the two scaled parameters of the soliton self-energy s' and t' and the scaled quark energy ϵ'_0 . Once this system has been solved, the product Ng^2 is determined from Eq. (3.9) by computing the normalization η' of the quark wavefunction in the scaled system. Clearly this determines the coupling constant g for a given number of particles N (or the number of quarks N for a given coupling constant g).

The asymptotic vacuum value of the soliton field σ_v has to be determined by an additional condition, e.g. by specifying the rms radius

$$\begin{aligned} r_{\text{rms}}^2 &= 4\pi \int r^4 (u_0^2 + v_0^2) dr = \\ &= \frac{4\pi}{(g\sigma_v)^2} \int r'^4 (u_0'^2 + v_0'^2) dr' / \eta' = \left(\frac{r'_{\text{rms}}}{g\sigma_v} \right)^2 \end{aligned} \quad (3.12)$$

or by specifying the total energy E_{tot} (Eq. (2.3))

$$\begin{aligned} E_{\text{tot}} &= N\epsilon_0 + 4\pi \int \left[\frac{1}{2} \left(\frac{d\sigma_0}{dr} \right)^2 + U(\sigma_0) \right] r^2 dr \\ &= \frac{\sigma_v}{g} E'_{\text{tot}} \end{aligned} \quad (3.13a)$$

where

$$E'_{\text{tot}} = \eta' \varepsilon'_0 + 4\pi \int \left[\frac{1}{2} \left(\frac{d\sigma'_0}{dr'} \right)^2 + U'(\sigma'_0) \right] r'^2 dr' \quad (3.13b)$$

Only after g has been determined can the parameters s and t of the soliton self energy function $U(\sigma)$ be found through Eq. (3.7) with the assumed values for s' and t' . It may seem strange to the reader that the parameters can only be determined after the solution of the problem. This inconvenience is offset by the simplicity in the solution of the scaled set of Eqs. (3.8) to (3.11), which has avoided the complication of solving an eigenvalue problem for the Dirac energies ε . [Our approach is similar to solving the quantum mechanical eigenvalue problem for a square well by declaring the eigenvalue a priori and then determining the parameters of the well that will support this eigenvalue.] The approach is particularly suitable for finding the general features of solutions for varying parameters as will be shown in the next sections.

IV. The Numerical Solution

We have solved the boundary value problem of the system of the Dirac Eqs. (3.8a and b) and the soliton Eq. (3.10) by applying the general purpose computer code COLSYS (COLlocation for SYStems) written by U. Ascher, J. Christiansen and R.D. Russell¹⁷⁻¹⁹. The code is able to handle up to 20 coupled ordinary differential equations of mixed order, with the highest order up to $m = 4$. The method of solution is a finite element method. The interval $[a,b]$, in which the differential equations have to be solved, is divided into a partition (mesh) $\pi: a = x_1 < x_2 < \dots < x_N < x_{N+1} = b$. The solution is approximated by piecewise polynomials $v \in P_{k+m, \pi} \cap C^{(m-1)}[a,b]$, i.e. v is a polynomial of order $k+m$ in each subinterval $I_i = (x_i, x_{i+1})$ of π and it is continuous to the order $m-1$ in the whole interval $[a,b]$. The piecewise polynomials are expressed in a basis of B-spline-functions.¹⁹ The collocation of the differential equations at k Gaussian points in each subinterval I_i together with the boundary conditions and the continuity condition leads

to a complete system of equations for the expansion parameters of the piecewise polynomials. In the case of nonlinear differential equations this is a nonlinear system of equations, which then is solved by a Newton method. The code COLSYS also includes a mesh selection algorithm, which aims to meet the required tolerances of the solution with the least number of meshpoints. It also produces reliable error estimates.

To solve our boundary value problem of Eqs. (3.8), (3.10) and (3.11), we have to introduce a cut-off radius R , which has to be chosen large enough, and we have to define the boundary conditions at this radius. Therefore the asymptotic behaviour of the Dirac components u'_0 and v'_0 and of the soliton field σ'_0 have to be examined for $r' \rightarrow \infty$. By putting $\sigma'_0 = 1$ for $r' \rightarrow \infty$ in Eqs. (3.8a and b) we get

$$u'_0(r' \rightarrow \infty) \propto \sqrt{\frac{\pi}{2\beta r'}} K_{1/2}(\beta r'), \quad v'_0(r' \rightarrow \infty) \propto \sqrt{\frac{\pi}{2\beta r'}} K_{3/2}(\beta r') \quad (4.1)$$

where $\beta^2 = 1 - \varepsilon'_0{}^2$, K_j is the modified spherical Bessel function of the third kind,²⁰ and

$$\frac{u'_0}{v'_0}(r' \rightarrow \infty) \approx \frac{(1+\varepsilon'_0)r'}{\beta r'+1} \approx \left(\frac{1+\varepsilon'_0}{1-\varepsilon'_0}\right)^{1/2} \quad (4.2)$$

The solution of Eq. (3.10) for $r' \rightarrow \infty$ can be found by putting $(u'^2 - v'^2)(r' \rightarrow \infty) = 0$. Then

$$\sigma'_0(r' \rightarrow \infty) \approx 1 - A \frac{\exp(-\alpha r')}{\alpha r'} \quad (4.3)$$

where $\alpha^2 = 2(s' + 3t')$.

Eqs. (3.8a and b) and (3.10) are then solved in the interval $r' \in [0, R]$ with the boundary conditions

$$v'_0(r'=0) = 0, \quad \frac{d\sigma'_0}{dr'}(r'=0) = 0 \quad (4.4)$$

$$\frac{u'_0(R)}{v'_0(R)} = \frac{(1+\varepsilon'_0)R}{\beta R+1}, \quad \sigma'_0(R) + \frac{R}{\alpha R+1} \frac{d\sigma'_0(R)}{dr'} = 1$$

V. Results for the Ground State

Since the main purpose of the present paper is to introduce the new numerical method for the solution of the mean-field equations of the Soliton Model and to show the advantages of this method, we will restrict the exploration in this section to the ground state solutions of the scaled equations (3.8) to (3.11). Furthermore the soliton self-energy $U(\sigma)$ (eq. 2.2) is restricted to $U(\sigma) = s\sigma^2(\sigma - \alpha_V)^2$, $t=0$, and the bare quark mass m is taken to be zero, as discussed above. This follows approximations made by Goldflam and Willets¹² and by Saly and Sundaresan¹³. The ground-state solution of the equations is defined by the condition that the Dirac components u and v are nodeless. This also corresponds to the solution with the lowest total energy for a given set of parameters $\{N, g, s\}$ or $\{\epsilon'_0, s'\}$.

The only parameters of the scaled soliton equations (3.8) and (3.10) are the quark energy ϵ'_0 and the parameter s' of the soliton self energy $U'(\sigma')$. The equations have been solved for a wide range in these parameters. Note that the scaled quark energy ϵ'_0 must be in the range $\epsilon'_0 \in (0, 1)$ for bound solutions of the quark equations. The parameter s' of the soliton self energy has been varied in the range of $s' = s/g^2 \in [0.01, 500]$.

Figure 3 shows the normalisation $\eta' = Ng^2$ (Eq. 3.9)) of the ground state solution as a function of ϵ'_0 for different values of the parameter s' . A striking feature of the results is the nearly power-law behaviour of η' with respect to ϵ'_0 for small ϵ'_0 . Although Fig. 3 only shows the results for $\epsilon'_0 \geq 0.1$, the equations have in fact been solved for $\epsilon'_0 \geq 0.01$. These results indicate a very accurate power-law of the form $\eta' \propto \epsilon'^{\alpha}_0$, with an exponent of $\alpha = -2.79$, which is nearly independent of s' . On the other hand, as ϵ'_0 increases to $\epsilon'_0 \rightarrow 1_-$, Friedberg & Lee^{8,11} showed that (for this three-space-dimensional case) the normalization $\eta' \rightarrow \infty$ and the total energy E'_{tot} approaches η' from above. All the curves in Fig. 3 show this rise in η' as $\epsilon'_0 \rightarrow 1_-$ - even that for $s' = 0.01$ (c.f. Table 1).

The total energy of the system $E'_{\text{tot}} = E_{\text{tot}}g/\sigma_v$ is shown in Fig. 4 versus the normalization $\eta' = Ng^2$. On each curve, given for constant parameters $s' = s/g^2$, there is defined a point S and a cusp (or spike^{8,11}) critical point C. The point S is defined by the condition that $E'_{\text{tot}} = \eta' \equiv \eta'_s$, i.e. the total energy is equal to the lowest energy for free quarks, $E'_{\text{PW}} \geq \eta'$. For $\eta' > \eta'_s$ the lower-energy soliton solution is stable. The critical cusp points C correspond to the minima $\eta'_c = \min \eta'$ (fixed s') of the curves in Fig. 3. For $\eta' < \eta'_c$ there exists no soliton solution of the equations. As has been deduced by Friedberg and Lee⁸, this feature is unique for the three-space-dimensional case and does not occur in lower dimensions. This is the first time, we believe, that these curves actually have been calculated for such a wide range of parameters. The values of the scaled quark energies ϵ'_0 , the normalization η' and the total energy E'_{tot} at the critical point C and at the point S are given in Table I for the parameters of s' that have been considered.

Note that Fig. 4 can be interpreted as a variation of the total energy with particle number N for a fixed coupling constant g . This is the way in which the solutions have been discussed by Friedberg and Lee^{8,11} for example. Then, because of the cusps, we find a critical particle number N_c below which the formalism does not support soliton solutions. Equally well we can interpret Fig. 4 as the variation of the total energy with coupling constant g for a fixed N . Then, again because of the cusps, we find a critical coupling constant g_c below which the formalism does not support soliton solutions for a given number of particles.

The computed soliton field σ'_0 and the two Dirac components u'_0 and v'_0 are plotted in Figs. 5 to 9 as functions of the scaled, dimensional radius r' . The figures show the variations of the solutions with the parameters ϵ'_0 and s' and also give the rms radii r'_{rms} for the quarks as computed from eq. (3.12). We make the following observations:

- a) The scaled radius of the soliton well decreases rapidly with increasing ϵ'_0 , while it depends little on the parameter s' . However, the diffuseness of the soliton well seems to depend only on s' : the well has a sharp

edge for large s' and is more diffuse for small s' . As ϵ'_0 is increased to 1 ($\epsilon'_0 \rightarrow 1_-$), the soliton well flattens out for small s' , as can be seen from Fig. 8 for $\epsilon'_0 = 0.9$ and $s' = 0.1$ and 0.01 ($\sigma' \rightarrow 1$ for all r').

b) The ratio of the lower Dirac component v'_0 to the upper component u'_0 decreases as ϵ'_0 increases, leading to a non-relativistic limit as $\epsilon'_0 \rightarrow 1_-$. For sufficient decrease of either of the parameters ϵ'_0 and s' the maxima of the upper Dirac component u'_0 change from the origin, $r'=0$, to finite radii $r'>0$.

c) Fig. 9 shows the results for the soliton field $\sigma'_0(r')$ and the Dirac components for an extreme example of small $\epsilon'_0 = 0.01$. In this figure the Dirac components u'_0 and v'_0 have been divided by $\sqrt{\eta'}$. It shows that for small values of s' the quark density is peaked at the surface of the soliton bag approaching the solution of the SLAC bag while for large values of s' the quarks are distributed in the whole volume of the bag as in the MIT bag. The derived quantities for $\epsilon'_0 = 0.01$ and for the different parameters of s' are summarized in Table II.

d) The rms radii r'_{rms} lie well inside the soliton well for small ϵ'_0 (Fig. 5), lie about at the edge of the soliton well for $\epsilon'_0 \approx 0.5$ (Fig. 7) and lie outside the radius of the soliton well for $\epsilon'_0 \rightarrow 1_-$ (Fig. 8). The variation of r'_{rms} with ϵ'_0 is also shown in Fig. 10. For small ϵ'_0 the radius r'_{rms} gets very large as also does the radius of the soliton well. On the other hand, as ϵ'_0 increases to $\epsilon'_0 \rightarrow 1_-$ the radius r'_{rms} also increases while the radius of the soliton well decreases. For $\epsilon'_0 \rightarrow 1$, the soliton field σ'_0 flattens out, approaching the unity it would reach in the limit of free quarks, where $E'_{tot} = \eta'$ (see Fig. 4).

e) Fig. 11 shows the variation in the contribution of the quark energy to the total energy E_{tot} ($N \epsilon'_0/E_{tot} = \eta' \epsilon'_0/E'_{tot}$). For small values of ϵ'_0 the ratio of the quark energy to the total energy $N \epsilon'_0/E_{tot}$ approaches the value in the MIT model (0.75) for large s' and that in the SLAC model (2/3) for small s' while for large $\epsilon'_0 \rightarrow 1_-$, the soliton energy vanishes and $E_{tot} \rightarrow N \epsilon'_0$.

One might like to compare the result obtained above for the soliton bag model with the experimental values of a three quark system,

e.g. the proton. Beside the total energy (Eq. (3.13) and the rms radius (Eq. (3.12)) we also calculate the magnetic moment μ , where

$$\mu' = \frac{8\pi}{3} \int_0^{\infty} r'^3 u' v' dr' / \eta' = g \sigma_V \mu \quad (5.1)$$

and the ratio of the axial-vector to the vector coupling-constant

$$g_A/g_V = \frac{20\pi}{3} \int_0^{\infty} r^2 (u^2 - \frac{1}{3} v^2) dr = \frac{20\pi}{3} \int_0^{\infty} r'^2 (u'^2 - \frac{1}{3} v'^2) dr' / \eta' \quad (5.2)$$

To compare theory with experiment, we form the dimensionless quantities

$$\frac{E_{\text{tot}} * r_{\text{rms}}}{N} = \frac{E'_{\text{tot}} * r'_{\text{rms}}}{\eta'}, \quad \frac{r_{\text{rms}}}{\mu} = \frac{r'_{\text{rms}}}{\mu'} \quad \text{and} \quad g_A/g_V$$

which are shown in Figs. (12a,b and c) as functions of ϵ'_0 , for different parameters of s' . For the adopted experimental values for the proton

$$E = 938.28 \text{ MeV} = 4.755 \text{ fm}^{-1}$$

$$r_{\text{rms}} = 0.83 \text{ fm}$$

$$\mu = 2.7928 \frac{e\hbar}{2m_p c} = .29368 \text{ efm} ,$$

the corresponding ratios are

$$\frac{E * r_{\text{rms}}}{N} = 1.3156, \quad \frac{r_{\text{rms}}}{\mu} = 2.8262$$

and

$$g_A/g_V = 1.25 .$$

The values are given in Figs. 12a, b and c as dashed lines.

The theoretical values of the ratios $E_{\text{tot}} * r_{\text{rms}}/N$ and r_{rms}/μ are above the experimental values for the proton for the values of ϵ'_0 that are shown. To match the experimental values, one would have to consider very small scaled quark energy $\epsilon'_0 \ll 0.1$. But for small ϵ'_0 the ratios of $E_{\text{tot}} * r_{\text{rms}}/N$ and r_{rms}/μ are nearly independent of the parameter s' of the soliton self energy. For very small ϵ'_0 and small s' one would reach

the limit of the SLAC-bag¹⁶, where the quark charge density lies near the surface of the bag. For small ϵ'_0 and large s' the limit is the MIT bag¹⁵ with sharp bag edges and the quark charge density distributed in the whole volume. The ratio of axial vector to vector coupling-constant g_A/g_V varies smoothly between $g_A/g_V \approx 0.6$ (for $\epsilon'_0 \ll 0.1$) to the non-relativistic quark value of $g_A/g_V = 5/3$ (for $\epsilon'_0 \rightarrow 1_-$). Clearly a fit to the experimental value of $g_A/g_V = 1.25$ would require a large ϵ'_0 (≈ 0.6) in disagreement with the other data.

At this stage we do not want to go into further details in the comparison of the theoretical results of the Soliton Bag Model with experiment. Before such detailed comparison one would have to explore the influence of a non-zero bare quark mass in the Lagrangian and of the parameter t in the soliton self energy. Furthermore one has to analyze the higher order corrections to the mean-field approximation.

In our opinion the most important modification to that given above is to extend the Lagrangian to make it chirally symmetric, as was proposed originally by Gell-Mann and Lévy¹ and applied extensively in Refs. 2-5, 14, 21-31. In the chiral invariant extension to the model the quarks interact with the soliton field σ and the isovector, pseudo-scalar π meson field. The advantage of this version of the soliton model³¹ is that most of the parameters of the model can be given a priori in terms of either known constants (e.g. pion mass, pion decay constant) or constants for which we might have some idea as to their relevant size (e.g. sigma mass). The coupled differential equations for the mean fields now have to be extended by the equations for the pion-fields. Birse and Banerjee¹⁴ have solved these equations for a hedgehog baryon following the method of solution of Goldflam and Willets¹². The same method outlined in Section 4 can be applied to this extended problem however. The results obtained for this chiral soliton model are being analysed by us in a systematic way and will be presented in a later paper.

VI. Excited States of the Soliton Model

Besides the ground state, which has been discussed in the previous section, the mean-field Eqs. (1.1) of the Soliton Model also have solutions for excited states of the Dirac Eq. (1.1a). We want to present here the results for some of these excited states, to demonstrate the great power of the numerical method of solving the equations.

a) Consider all quarks in the same $s_{1/2}$ -state ($\ell=0$, $j=1/2$).

We first show results for the excited states of the system of Eqs. (1.1) or the scaled Eqs. (3.8) to (3.10). The solutions are labelled by ns , where n is the number of nodes of the large Dirac component u and s stands for $\ell=0$. The scaled quark energy ϵ'_0 has been chosen in these calculations to give a constant normalization of $\eta' = Ng^2 = 3000$, and the parameter s' of the soliton self energy has been taken as $s'=0.5$. Fig. 13 shows the solutions for these parameters for the $0s$, $1s$ and $2s$ states. The scaled size of the soliton well increases with the node number n and the surface diffuseness stays constant, although it gets a pronounced internal structure. The lower part of Fig. 13 gives the large and small Dirac components u' and v' as well as the rms radii r'_{rms} .

b) All quarks in the same $p_{1/2}$ state ($\ell=1$, $j=1/2$).

Instead of using the ground state Dirac wavefunction ϕ_0 (3.1), one can assume that all the quarks are in an excited odd parity p state with angular momenta $\ell=1$, $j=1/2$

$$\phi_1 = \begin{pmatrix} u_1(r) \hat{\sigma} \cdot \hat{r} \\ i v_1(r) \end{pmatrix} s \quad (6.1)$$

The scaled mean-field equations in radial coordinates read then

$$\frac{du_1}{dr'} = - \frac{2}{r'} u_1' - (\epsilon_1' + \alpha_1') v_1 \quad (6.2a)$$

$$\frac{dv_1'}{dr'} = + (\epsilon_1' - \alpha_1') u_1' \quad (6.2b)$$

and

$$\frac{d^2\sigma_1'}{dr'^2} = -\frac{2}{r'} \frac{d\sigma_1'}{dr'} + \frac{dU'(\sigma_1')}{d\sigma_1'} + (u_1'^2 - v_1'^2) \quad (6.3)$$

and the normalization is as in eq. (3.9)

$$4\pi \int r'^2 (u_1'^2 + v_1'^2) dr' = \eta' = Ng^2 \quad (6.4)$$

The boundary conditions for u_1' , v_1' and σ_1' are

$$u_1'(r'=0) = 0, \quad v_1'(r'=\infty) = 0, \quad \sigma_1'(r'=\infty) = 1, \quad \frac{d\sigma_1'}{dr'}(r'=0) = 0. \quad (6.5)$$

The three lowest solution with all quarks occupying the states 0p, 1p or 2p, of Eqs. (6.2) to (6.5) are shown in Fig. 14. The scaled quark energies ε_1' have again been adjusted for a constant normalization of $\eta' = Ng^2 = 3000$ and s' is again taken as $s' = 0.5$. Table III lists the quark energies ε' , the total energies E'_{tot} and the rms radii r'_{rms} for the above excited s- and p-states. It gives the scaled quantities as well as the energies in units of the vacuum soliton field α_v for the case of three quarks, i.e. $N = 3$, $g^2 = 1000$. Note the nearly linear increase of the single particle energies with varying nodes for both the s-orbit and the p-orbit occupancy reminiscent of the solutions for a non-relativistic oscillator.

c) Quarks in different states.

Finally we want to show the solution of the mean-field equations for the case where two different states ϕ_{k_1} and ϕ_{k_2} are occupied by the quarks. Only spherically symmetric solutions are considered, i.e. $j_1 = j_2 = 1/2$. In this case one has to solve the boundary value problem of the following system of differential equations, written in radial coordinates in the scaled quantities according to Eqs. (3.6), (3.7)

$$\frac{du_i'}{dr'} = -\frac{(1+\kappa_i)}{r'} u_i' - (\varepsilon_i' + \sigma') v_i' \quad (6.6a)$$

$$i = 1, 2$$

$$\frac{dv_i'}{dr'} = -\frac{(1-\kappa_i)}{r'} v_i' + (\varepsilon_i' - \sigma') u_i' \quad (6.6b)$$

and

$$\frac{d^2 \sigma'}{dr'^2} = -\frac{2}{r'} \frac{d\sigma'}{dr'} + \frac{dU'(\sigma')}{d\sigma'} + (u_1'^2 - v_1'^2) + (u_2'^2 - v_2'^2) \quad (6.7)$$

where

$$\kappa_i = \begin{cases} -(\ell+1) & \text{for } j = \ell+1/2 \\ +\ell & \text{for } j = \ell-1/2 \end{cases} = \begin{cases} -1 & \text{for } s_{1/2} \text{ states} \\ +1 & \text{for } p_{1/2} \text{ states} \end{cases}$$

The boundary conditions are

$$\begin{aligned} v'(r'=0) = 0, \quad u'(r'=\infty) = 0 & \quad \text{for } s_{1/2} \text{ states} \\ u'(r'=0) = 0, \quad u'(r'=\infty) = 0 & \quad \text{for } p_{1/2} \text{ states} \end{aligned} \quad (6.8a)$$

and

$$\frac{d\sigma'}{dr'}(r=0) = 0, \quad \sigma'(r=\infty) = 1 \quad (6.8b)$$

The normalizations of the Dirac wavefunctions ϕ_{k_1} and ϕ_{k_2} are

$$4\pi \int r'^2 (u_i'^2 + v_i'^2) dr' = \eta_i' = N_i g^2 \quad i = 1, 2 \quad (6.9)$$

We take a system of 3 quarks with a coupling constant of $g^2 = 1000$ and a parameter of the soliton self energy of $s = s'g^2 = 500$, $s' = 0.5$. We further put 2 quarks in the state ϕ_{k_1} and 1 quark in the state ϕ_{k_2} , i.e. the normalization of the scaled wavefunctions have to be $\eta_1' = N_1 g^2 = 2000$ and $\eta_2' = N_2 g^2 = 1000$. To fulfill the above side conditions of the normalization, the scaled energies ϵ_1' and ϵ_2' have to be iterated. It is found that about five iterations are sufficient to reach an accuracy in the normalization of 10^{-3} . The solutions are shown in Figs. 15 and 16 for the cases of $k_1 = 0s$, $k_2 = 0p$ and $k_1 = 0s$, $k_2 = 1s$ respectively, and the corresponding energies and rms radii are listed in Table IV. A comparison of Figs. 14 and 15 with Figs. 12 and 13 shows that the soliton field σ in the above case is approximately a two to one superposition of the corresponding soliton fields in the cases of section 6a) and 6b) respectively. The wavefunctions of the quarks in the ground state, u_1' and v_1' , are pushed towards larger radii, with a large rms

radius, while the rms radius of the excited quark in the $0p$ or $1s$ state, respectively, is relatively small.

VII. Summary and Conclusions

We have presented a new numerical approach to the solution of the soliton bag model of Friedberg and Lee. The method is particularly suitable for exhibiting the general properties of the model for various parameter choices. We have shown the general features of the model for degenerate minimum energy of the soliton self energy ($t=0$) and for variation in (effectively) the parameter s , coupling constant g and particle number N . We have considered examples when all quarks occupy the $ns_{1/2}$ or $np_{1/2}$ -orbits ($n=0,1,2$) or when two occupy the $0s_{1/2}$ and one the $1s_{1/2}$ or $0p_{1/2}$ orbits. We show how the results of the model, for various observables, compare with those of the proton by considering dimensionless products. We have refrained from a detailed comparison, however, since we believe that the model must be extended to a chirally symmetric model by the addition of pion fields. This latter addition, and the consequent predictions of the model following the methods of this paper, will form the subject of a subsequent paper. Consideration of recoil corrections must also be given as in ref. 32.

Numerical solutions of the Friedberg-Lee model have been found by Goldflam and Willets¹² and Saly and Sundaresan¹³ for particular sets of parameters using a different numerical method. These solutions have been indicated by circles and pluses respectively on Fig. 3. The results from our method agree with those from refs. 12 and 13 for the same parameters. It is clear from our own analysis that the previous method failed to find solutions at times because parameters had been chosen beyond the critical values which, as explained in the text, determine when the formalism will or will not support soliton solutions.

We conclude from our study that treating the equations of motion as a set of coupled differential equations and then using the computer code COLSYS has many advantages over other methods and certainly

illuminates general features. We are finding that it is a straightforward extension to include the pion field in a chirally symmetric version of the model.

Acknowledgements

It is a pleasure to thank L. Wilets, R. Saly and M.K. Sundaresan for frank discussions on the soliton model. We acknowledge use of the computer code COLSYS and thank its authors U. Ascher, J. Christiansen and R.D. Russell for making it available to us. The help and advice of D. Duncan in use of the COLSYS program is gratefully acknowledged. This work is an outgrowth of that by H. Vogel who was applying yet another method of solution. We wish to thank Mr. Vogel for freely supplying his available numerical solutions for use in checking. One of us (Th. K) acknowledges receipt of a Natural Sciences & Engineering Research Council of Canada Post-Doctoral Fellowship and the hospitality at the Chalk River Nuclear Laboratories.

Note added

After finishing this paper we have learned of the work of S. Kahana, G. Ripka and V. Soni³³. They solve the equations of motion of the chirally symmetric soliton model for the hedgehog state by diagonalizing the Hamiltonian in a finite basis. The same numerical method given in this paper has also been applied to get these hedgehog solutions. The results will be reported in a forthcoming paper.

References

1. M. Gell-Mann and M. Levy, The Axial Vector Current in Beta Decay, II Nuovo Cimento 16(1960)705.
2. T.H.R. Skyrme, A Non-linear Field Theory, Proc. Roy. Soc. 260(1961)127.
3. T.H.R. Skyrme, Particle States of a Quantized Meson Field, Proc. Roy. Soc. 262(1961)237.
4. J.K. Perring and T.H.R. Skyrme, A Model Unified Field Equation, Nuclear Physics 31(1962)550.
5. T.H.R. Skyrme, A Unified Field Theory of Mesons and Baryons, Nuclear Physics 31(1962)556.
6. M. Creutz, Quark "Bags" and Local Field Theory, Phys. Rev. D 10(1974)1749.
7. M. Creutz and K.S. Soh, Quark Bags and Local Field Theory. II. Confinement of Fermi and Vector Fields, Phys. Rev. D 12(1975)443.
8. R. Friedberg and T.D. Lee, Fermion-field Nontopological Solitons, Phys. Rev. D 15(1977)1694.
9. R. Friedberg and T.D. Lee, Fermion-field Nontopological Solitons. II. Models for Hadrons, Phys. Rev. D 16(1977)1096.
10. R. Friedberg and T.D. Lee, Quantum Chromodynamics and the Soliton Model of Hadrons, Phys. Rev. D 18(1978)2623.
11. T.D. Lee, "Particle Physics and Introduction to Field Theory", Harwood Academic Publishers, Chur, London, New York, 1981.
12. R. Goldflam and L. Willets, Soliton Bag Model, Phys. Rev. D 25(1982)1951.
13. R. Saly and M.K. Sundaresan, Excited States in the Soliton Bag Model, Phys. Rev. D 29(1984)525; R. Saly, Soliton Bag Model, Comput. Phys. Commun. 30(1983)411.
14. M.C. Birse and M.K. Banerjee, A Chiral Soliton Model of Nucleon and Delta, Phys. Lett. 136B(1984)284.
15. A. Chodos, R.L. Jaffe, K. Johnson, C.B. Thorn and V.F. Weisskopf, New extended model of hadrons (MIT-bag), Phys. Rev. D 9(1974)3471. T. DeGrand, R.L. Jaffe, K. Johnson, and J. Kiskis, Masses and Other Parameters of the Light Hadrons, Phys. Rev. D 12(1975)2060.
16. W.A. Bardeen, M.S. Chanowitz, S.D. Drell, M. Weinstein and T.-M. Yan, Heavy quarks and strong binding: A field theory of hadron structure (SLAC - bag), Phys. Rev. D 11(1975)1094.
17. U. Ascher, J. Christiansen and R.D. Russell, A Collocation Solver for Mixed Order Systems of Boundary Value Problems, Math. Comp. 33(1979)659.

18. U. Ascher, J. Christiansen and R.D. Russell, COLSYS - A Collocation Code for Boundary Value Problems, Proc. Conf. for Codes for BVP's in ODE's, Houston, Texas, 1978.
19. C. DeBoor, Package for Calculating with B-Splines, SIAM J. Numer. Anal. 14(1977)441.
20. "Handbook of Mathematical Functions", edited by M. Abramowitz and I.A. Stegun, Dover, New York, 1965.
21. A. Chodos and C.B. Thorn, Chiral Invariance in a Bag Theory, Phys. Rev. D 12(1975)2733.
22. V. Vento, M. Rho, E.N. Nyman, J.H. Jun and G.E. Brown, Chiral Pion Dynamics for Spherical Nucleon Bags, Nucl. Phys. A345(1980)413.
23. A.P. Balachandran, V.P. Nair, S.G. Rajeev and A. Stern, Soliton States in the Quantum-chromodynamic Effective Lagrangian, Phys. Rev. D 27(1983)1153.
24. E. Witten, Global Aspects of Current Algebra, Nucl. Phys. B223(1983)422.
25. E. Witten, Current Algebra, Baryons, and Quark Confinement, Nucl. Phys. B 223(1983)433.
26. G.S. Adkins, C.R. Nappi, and E. Witten, Static Properties of Nucleons in the Skyrme Model, Nucl. Phys. B228(1983)552.
27. M. Rho, A.S. Goldhaber and G.E. Brown, Topological Soliton Bag Model for Baryons, Phys. Rev. Lett. 51(1983)747.
28. J. Goldstone and F. Wilczek, Fractional Quantum Numbers on Solitons, Phys. Rev. Lett. 47(1981)986.
29. J. Goldstone and R.L. Jaffe, Baryon Number in Chiral Bag Models, Phys. Rev. Lett. 51(1983)1518.
30. M. Rho, Nucleon as a Topological Soliton, Lectures given at the International School of Nuclear Physics, Erice (Sicily), Italy, 6-18 April, 1983.
31. A.W. Thomas, Chiral Symmetry and the Bag Model: A New Starting Point for Nuclear Physics, Advances in Nuclear Physics, Vol. 13, Chapter 1, Edited by J.W. Negele and E.W. Vogt, Plenum Press, New York-London, 1984.
32. J.-L. Dethier, R. Goldflam, E.M. Henley and L. Wilets, Recoil Corrections in Bag Models, Phys. Rev. D27(1983)2191.
33. S. Kahana, G. Ripka and V. Soni, Soliton with Valence Quarks in the Chiral Invariant σ Model, Nucl. Phys. A415(198)351.

Table I. The scaled values of the quark energy ϵ'_0 , the normalization η' and the total energy E'_{tot} are given at the point S and at the critical cusp point C for the specified values of the parameters s' of the soliton self energy. (Compare with Figs. 3 and 4).

s'	ϵ'_s	$\eta'_s = E'_{\text{tots}}$	ϵ'_c	η'_c	E'_{totc}
500.0	.733	1179.0	.938	653.1	754.4
100.0	.733	525.5	.937	293.5	338.5
50.0	.732	372.1	.935	209.4	241.2
10.0	.729	171.4	.927	101.0	115.1
5.0	.729	125.4	.920	77.47	87.20
1.0	.743	65.82	.891	50.24	53.43
0.5	.771	51.25	.898	43.02	44.54
0.1	.908	27.37	.967	25.20	25.34
0.05	.953	19.94	.983	18.56	18.61
0.01	.990	9.200	.997	8.580	8.584

Table II. Results obtained for the extremely small scaled quark energy of $\epsilon'_0 = 0.01$ and for the values 10.0, 1.0, 0.1 and 0.01 of the self energy parameter s' . (Compare with Fig. 9).

$\epsilon'_0 = 0.01$	$s' =$	10.0	1.0	0.1	0.01
Normalization η'		33.6242×10^6	8.84923×10^6	2.50884×10^6	0.808548×10^6
Total Energy E'_{tot}		523095.	137017.	38888.9	12773.6
r'_{rms}		107.3	103.7	101.8	101.0
μ'_p		35.01	34.21	33.76	33.57
g_A/g_V		.6677	.6141	.5846	.5713

rescaled for $N = 3$, $E_{tot} = M = 1$ GeV

ϵ_0 [MeV]	214.26	215.28	215.04	210.99
r_{rms} [fm]	.9885	.9509	.9345	.9447
μ_p (2M/e)	3.268	3.178	3.141	3.182

Table III. The scaled values of the quark energy ϵ' , the total energy E'_{tot} and the root mean square radii r'_{rms} for the excited state where all quark occupy the same $ns_{1/2}$ -state or $np_{1/2}$ -state for $\eta' = Ng^2 = 3000$ and $s' = 0.5$. The energies are also given in units of the vacuum value σ_v of the soliton field for $N = 3$, $g^2 = 1000$ and $s = 500$. (Compare with Figs. 12 and 13).

$\eta' = Ng^2 = 3000, s' = 0.5$				$N=3, g^2 = 1000., s = 500$	
state	ϵ'	E'_{tot}	r'_{rms}	ϵ/σ_v	E_{tot}/σ_v
0s	.154016	734.709	7.81310	4.87040	23.2336
0p	.235246	1126.52	7.42429	7.43914	35.8239
1s	.306613	1462.13	8.36742	9.69594	46.2365
1p	.373496	1750.37	9.47218	11.8110	55.3517
2s	.437215	2029.75	10.3117	13.8260	64.1865
2p	.496751	2275.33	11.1878	15.7087	71.9523
3s	.554550	2518.43	11.8826	17.5364	79.6397

Table IV. The scaled values of the quark energies ϵ_1' and ϵ_2' , the total energy E_{tot}' and the root mean square radii $r_{\text{rms}1}'$ and $r_{\text{rms}2}'$ for the case where 2 quarks are assumed to occupy the ground state $0s_{1/2}$ -state (ϵ_1') and 1 quark the $0p_{1/2}$ -state or the $1s_{1/2}$ -state (ϵ_2') for $g^2 = 1000$ and $s' = 0.5$. The energies are also given in units of σ_v . (Compare with Figs. 14 and 15).

state		$\eta_1' = N_1 g^2 = 2000. \quad s' = 0.5$					$N_1=2$	$g^2=1000.$	$s=500.$
		$\eta_2' = N_2 g^2 = 1000.$					$N_2=1$		
k1	k2	ϵ_1'	ϵ_2'	E_{tot}'	$r_{\text{rms}1}'$	$r_{\text{rms}2}'$	ϵ_1'/σ_v	ϵ_2'/σ_v	E_{tot}'/σ_v
0s	0p	.151819	.285733	933.144	9.00953	6.20387	4.80094	9.03568	29.5086
0s	1s	.140763	.412669	1063.39	9.30778	7.68587	4.45132	13.0498	33.6275

Fig. 1. General structure of the soliton self energy function $U(\sigma) = (\sigma - \sigma_v)^2 (s\sigma^2 + 2t\sigma_v\sigma + t\sigma_v^2)$ for $t = 0, \frac{1}{9}s, \frac{2}{9}s$ and $\frac{1}{3}s$. The minimum A is $U(\sigma = 0) = t\sigma_v^4$ and the barrier height B at $\sigma_M = \sigma_v(s-3t)/2s$ is $U(\sigma_M) = \frac{\sigma_v^4(3t+s)^2(s^2 + 2ts - 3t^2)}{16s^3}$.

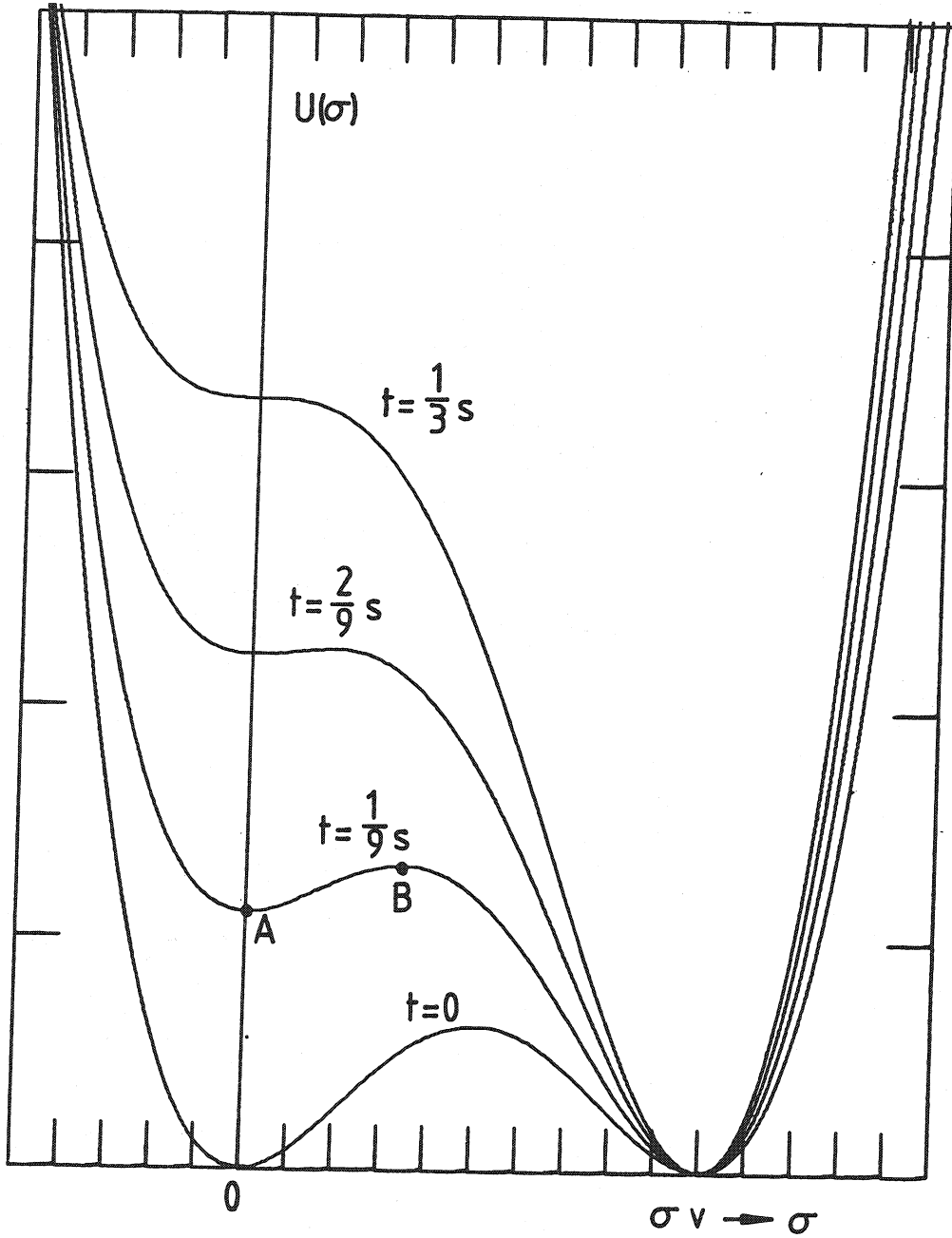


Figure 1

Fig. 2. General structure of the soliton mean field $\sigma(r)$.

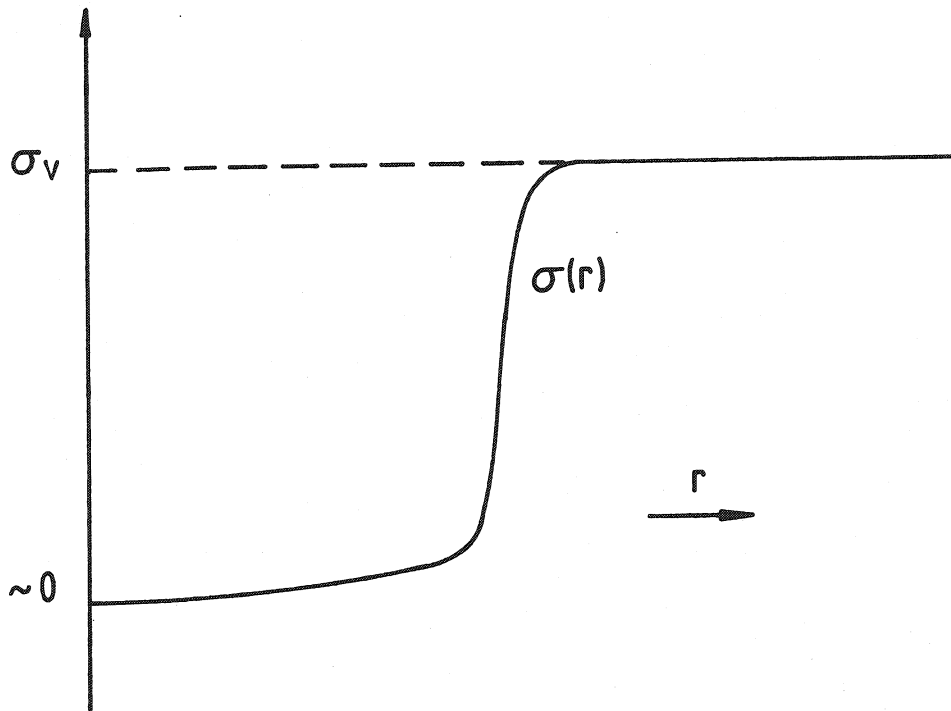


Figure 2

Fig. 3. General structure of the normalization $\eta' = Ng^2$ (Eq. 3.10) as a function of $\epsilon'_0 = \epsilon_0/g\sigma_v$ (Eq. 3.6) for the values of $s' = s/g^2 = 500., 100., 50., 10., 5., 1., 0.5, 0.1, 0.05$ and 0.01 and $t'=0$. Note the logarithmic scales. Solutions found by Goldflam & Wilets¹² (o) and by Saly & Sundaresan¹³ (+) for specific parameters are indicated.

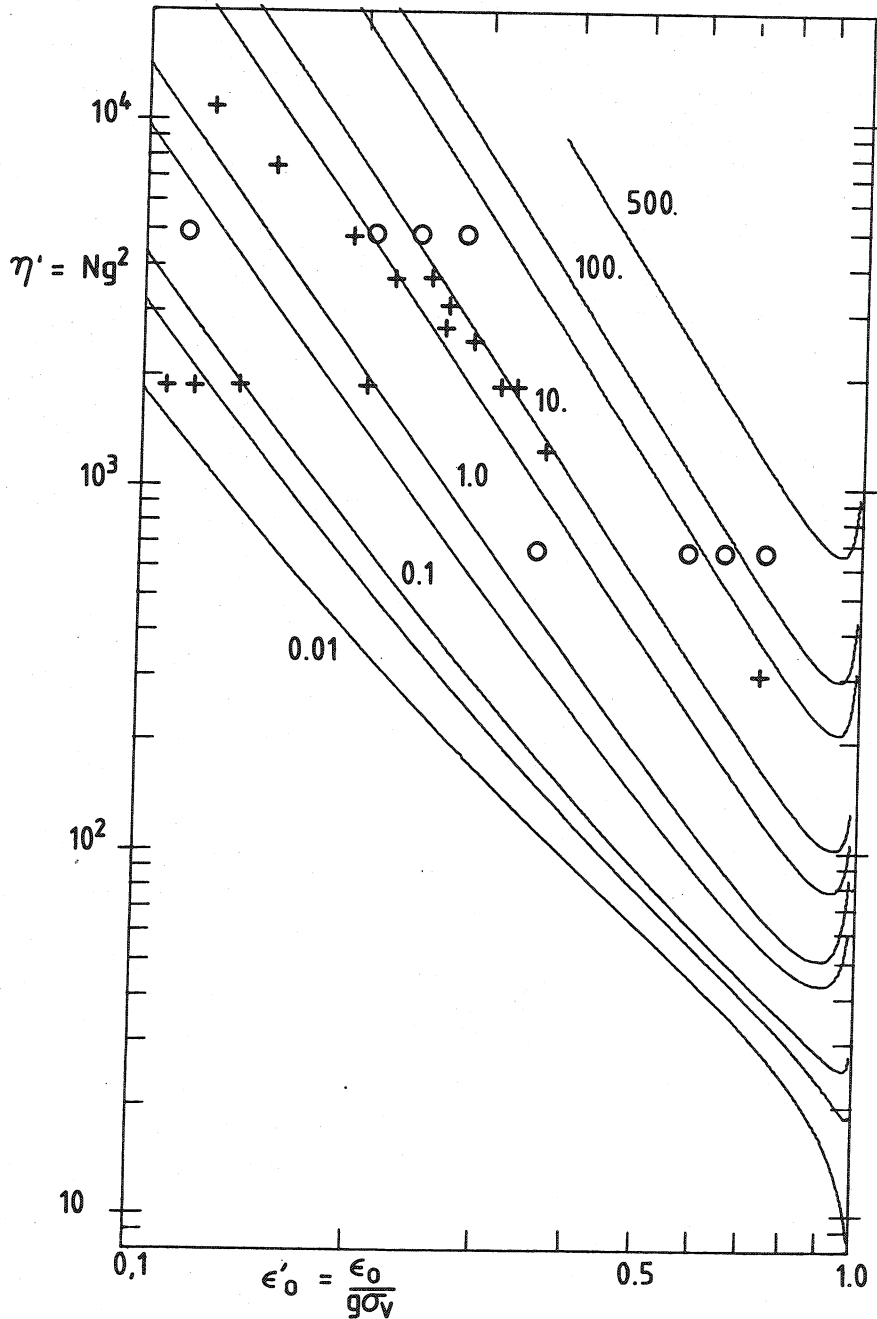


Figure 3

Fig. 4. General structure of the scaled total energy $E'_{tot} = \frac{g}{\sigma_v} E_{tot}$ (Eq. 3.12a) as a function of $\eta' = Ng^2$ for the values of s' considered in Fig. 3. The critical point C and the point S have been labelled only for the values $s' = 10$ and $s' = 100$.

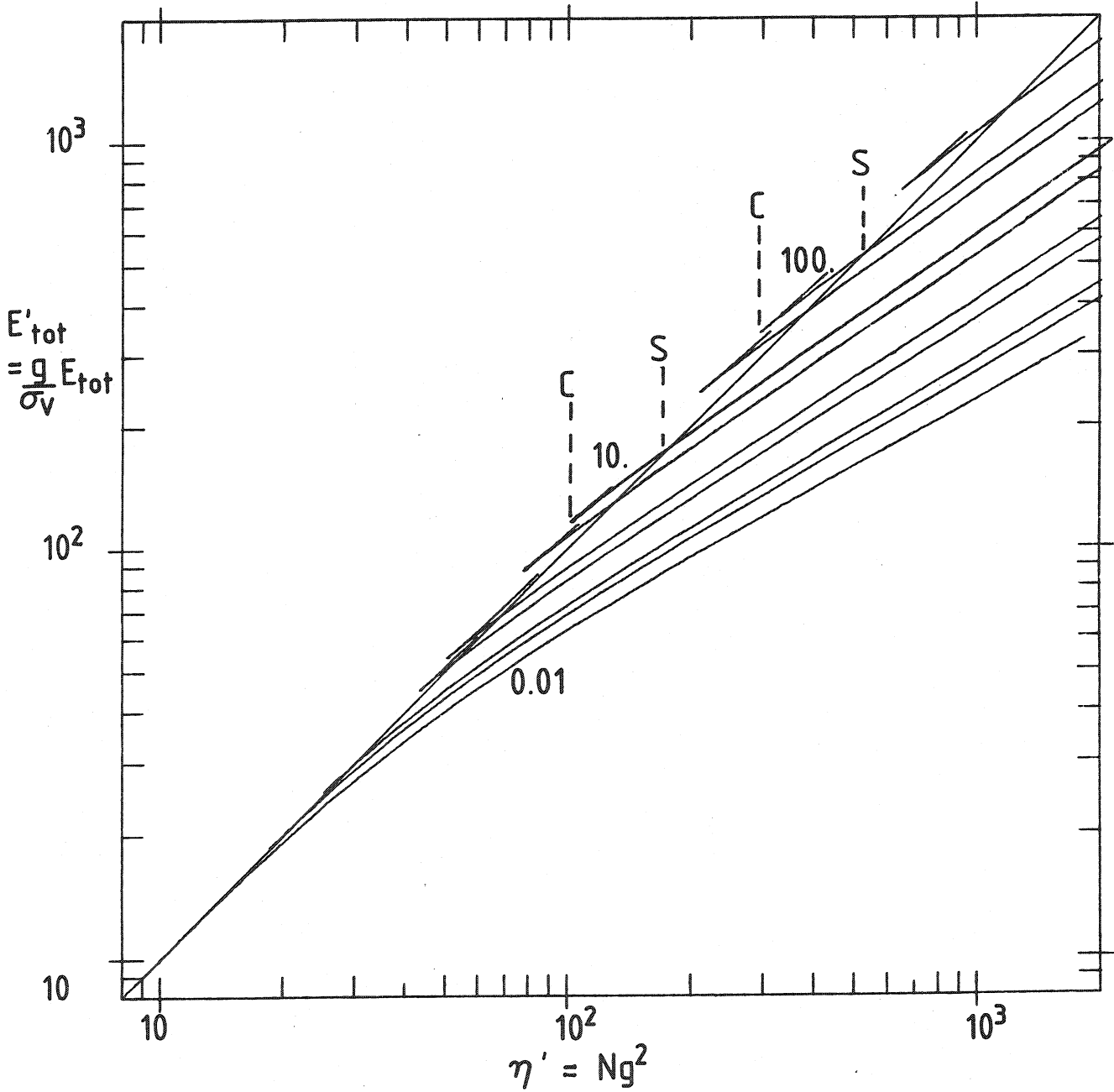


Figure 4

Fig. 5. At the top is shown the scaled soliton field $\sigma'_0(r')$ as a function of the scaled radius r' for the values of $s' = 10.00$ (1), 1.00 (2), 0.10 (3) and 0.01 (4). The bottom curves show the corresponding solutions of the scaled upper radial function $u'_0(r')$ (solid curves) and the lower function $v'_0(r')$ (dashed curves) as a function of r' . The root mean square radii r'_{rms} for the solutions are also shown. All solutions are for the scaled quark energy $\epsilon'_0 = 0.1$.

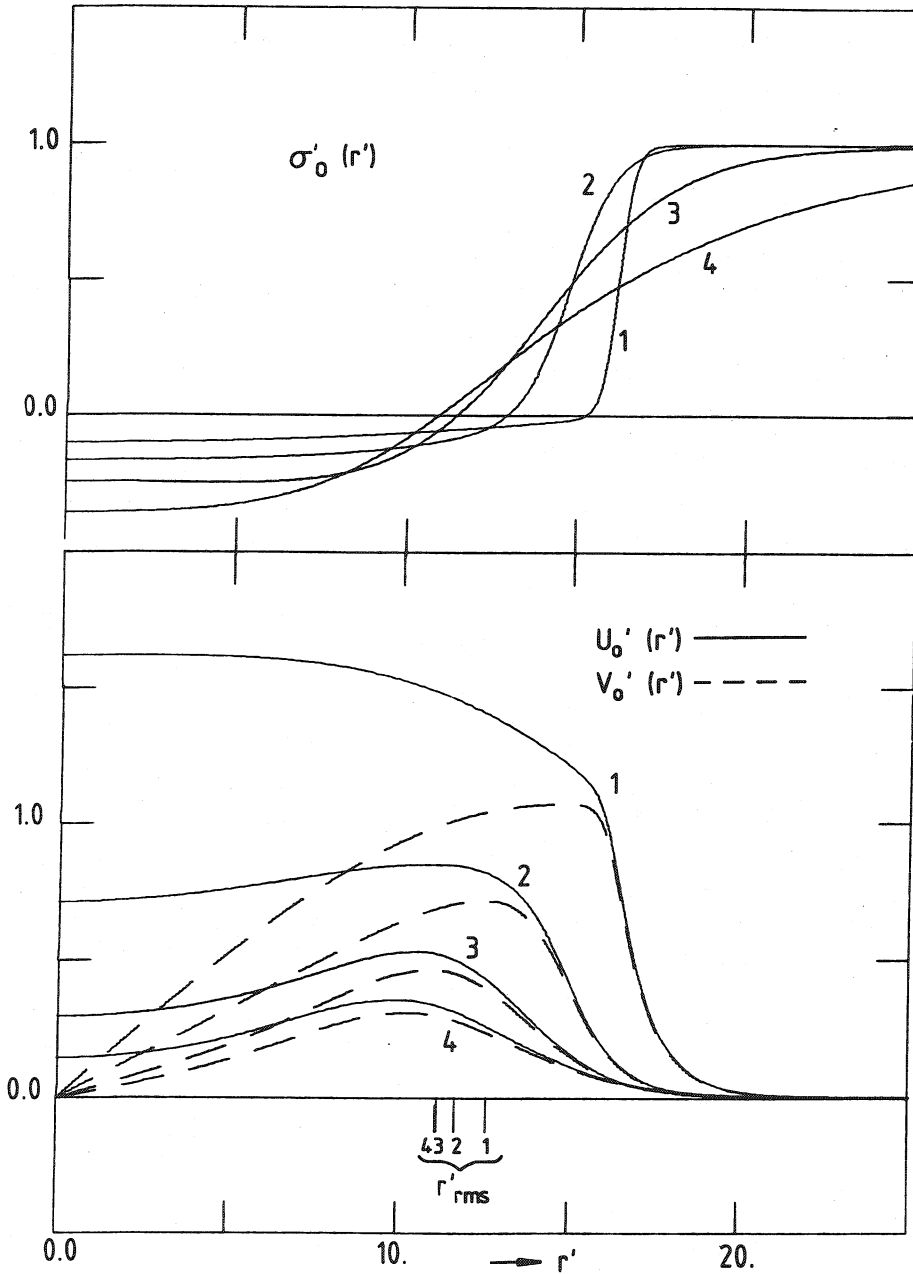


Figure 5

Fig. 6. As in Fig. 5 but for $\epsilon'_0 = 0.2$.

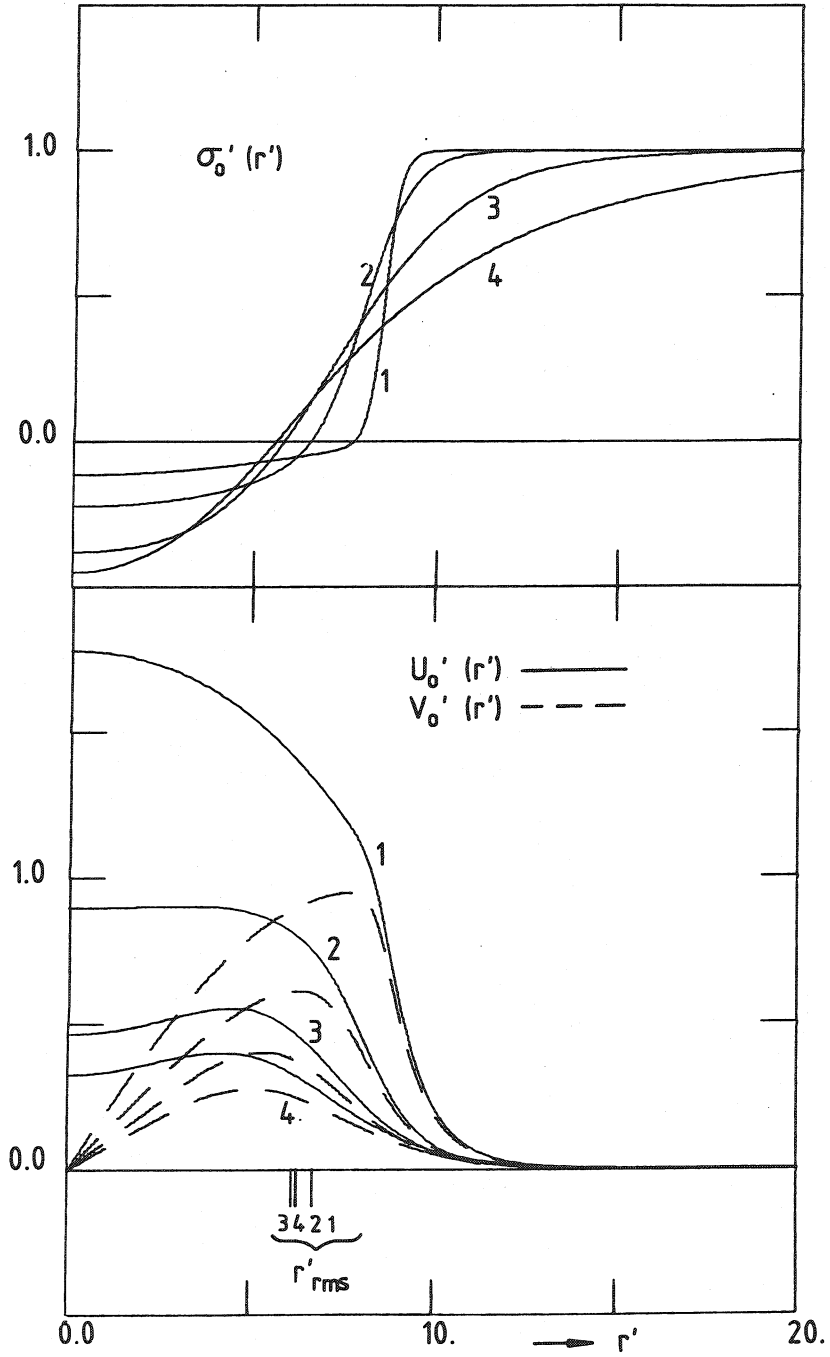


Figure 6

Fig. 7. As in Fig. 5 but for $\epsilon'_0 = 0.5$.

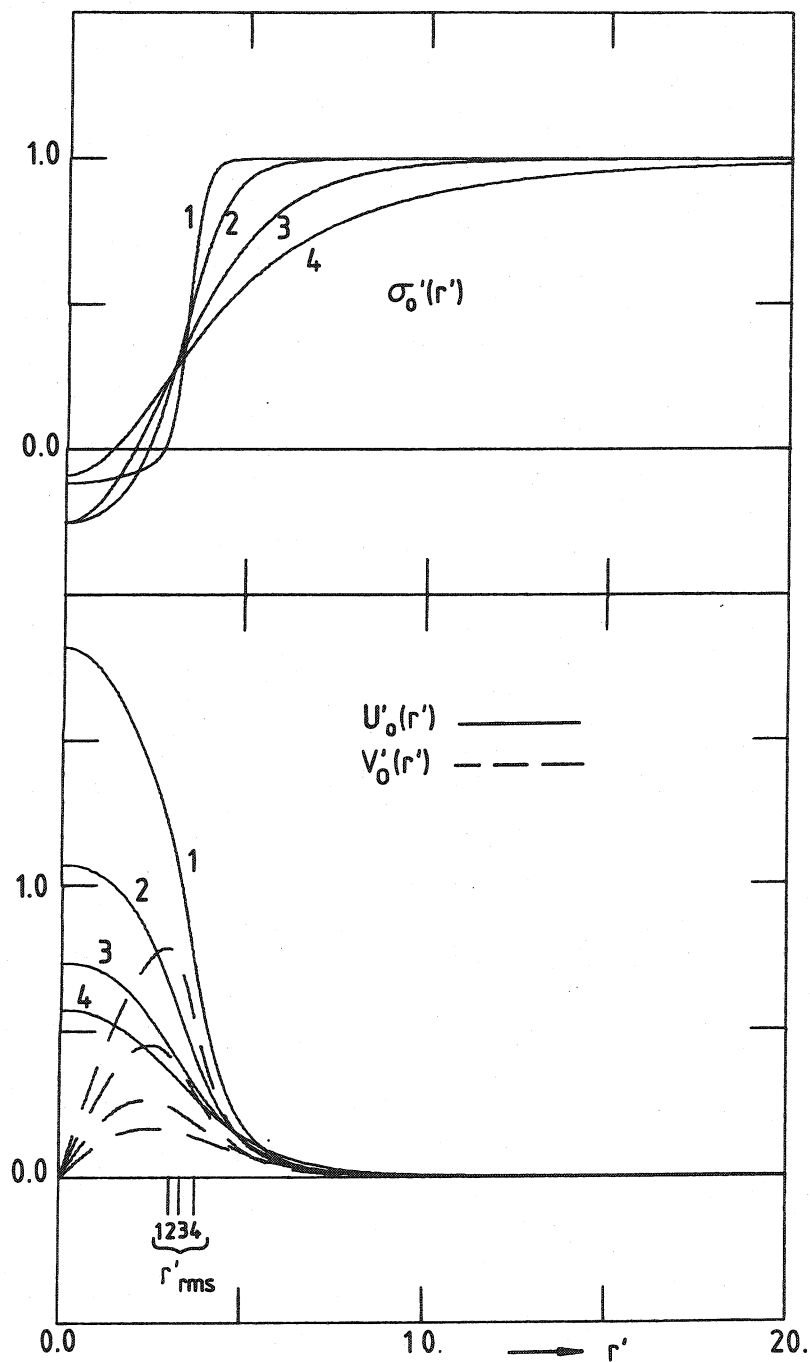


Figure 7

Fig. 8. As in Fig. 5 but for $\epsilon'_0 = 0.9$.

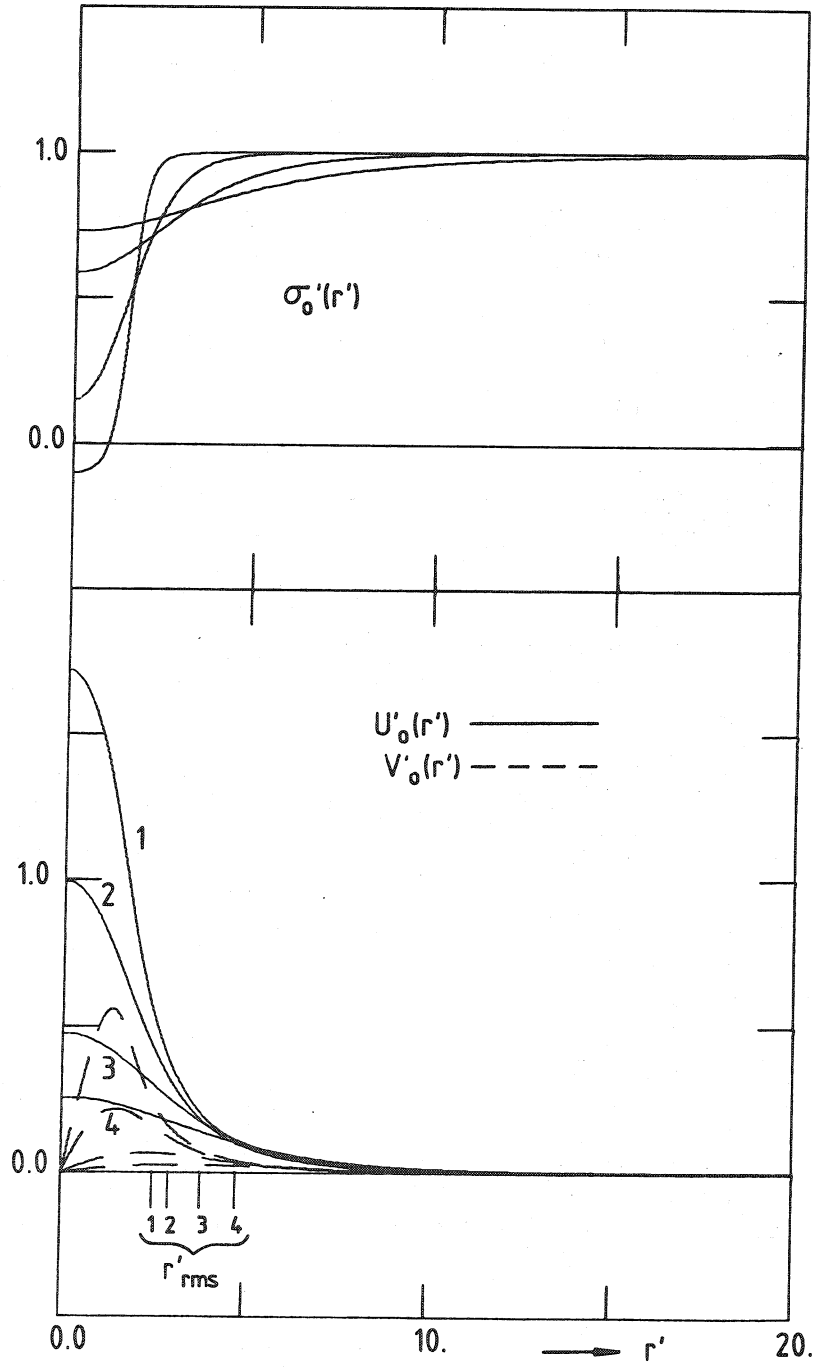


Figure 8

Fig. 9. As in Fig. 5 but for extremely small $\epsilon'_0 = 0.01$ showing the tendency towards an MIT bag (large s') and a SLAC bag (small s'). The Dirac components u'_0 and v'_0 have been divided by the corresponding $\sqrt{\eta'}$. Derived quantities are given in Table II.

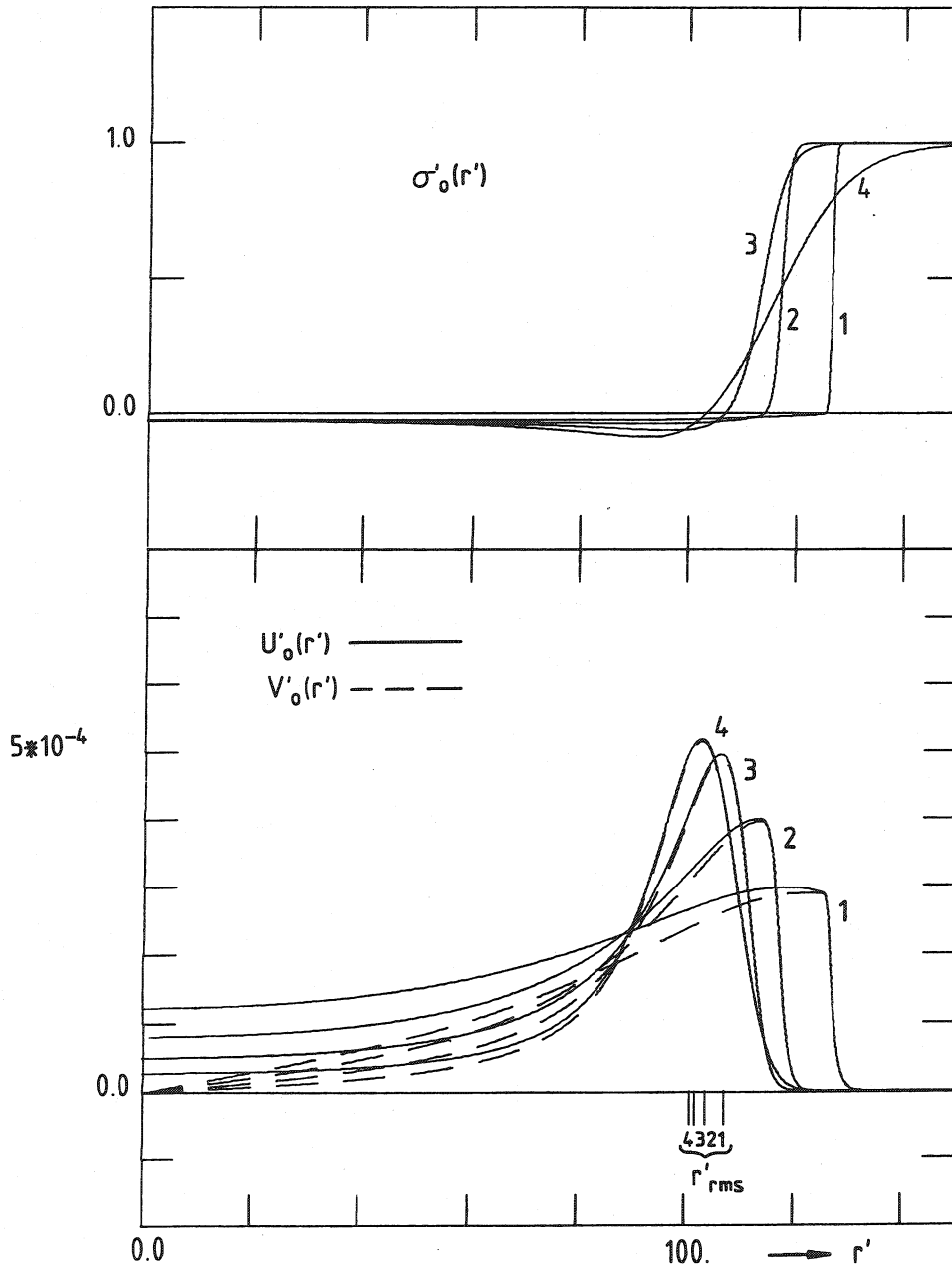


Figure 9

Fig. 10. The root mean square radii r'_{rms} shown as a function of ϵ' for $s' = 0.01, 0.1, 1.0, 10.0$ and 100.0 .

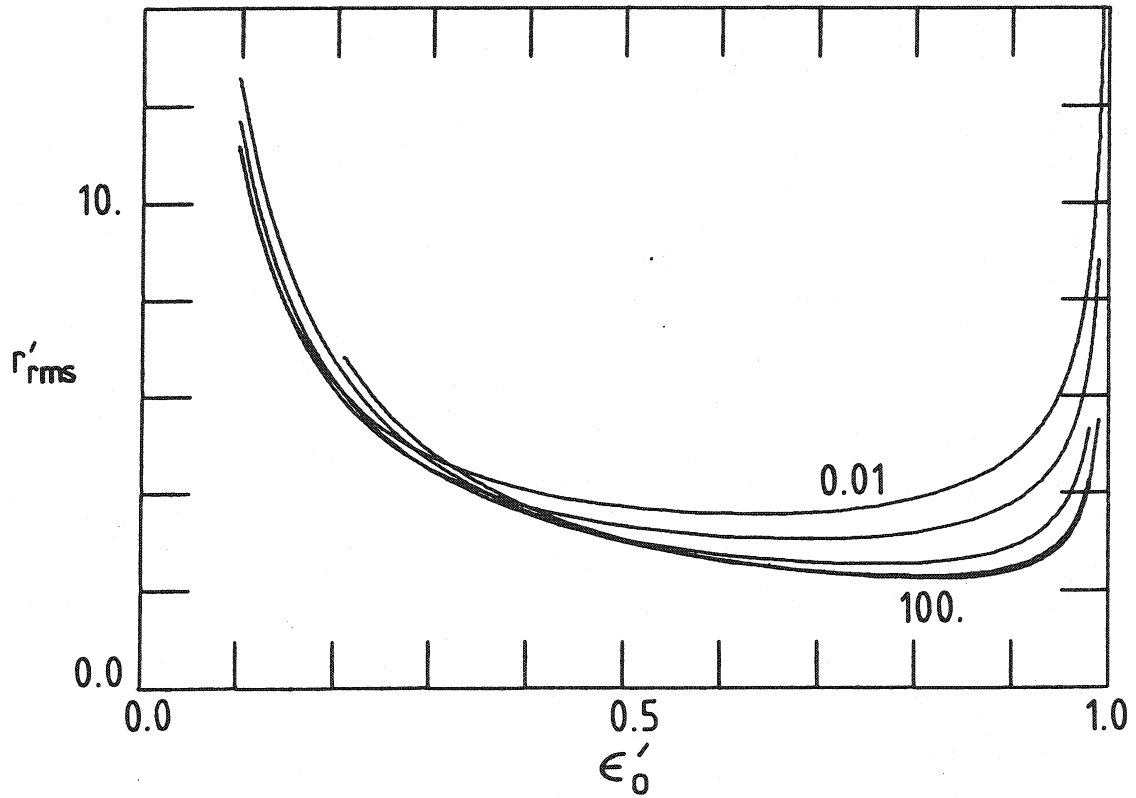


Figure 10

Fig. 11. The ratio of the quark energy $N\epsilon$ to the total energy E_{tot} as a function of ϵ' . Note $\frac{N\epsilon}{E_{tot}} = \frac{\eta'\epsilon'}{E'_{tot}}$ and hence is computed only in terms of scaled quantities.

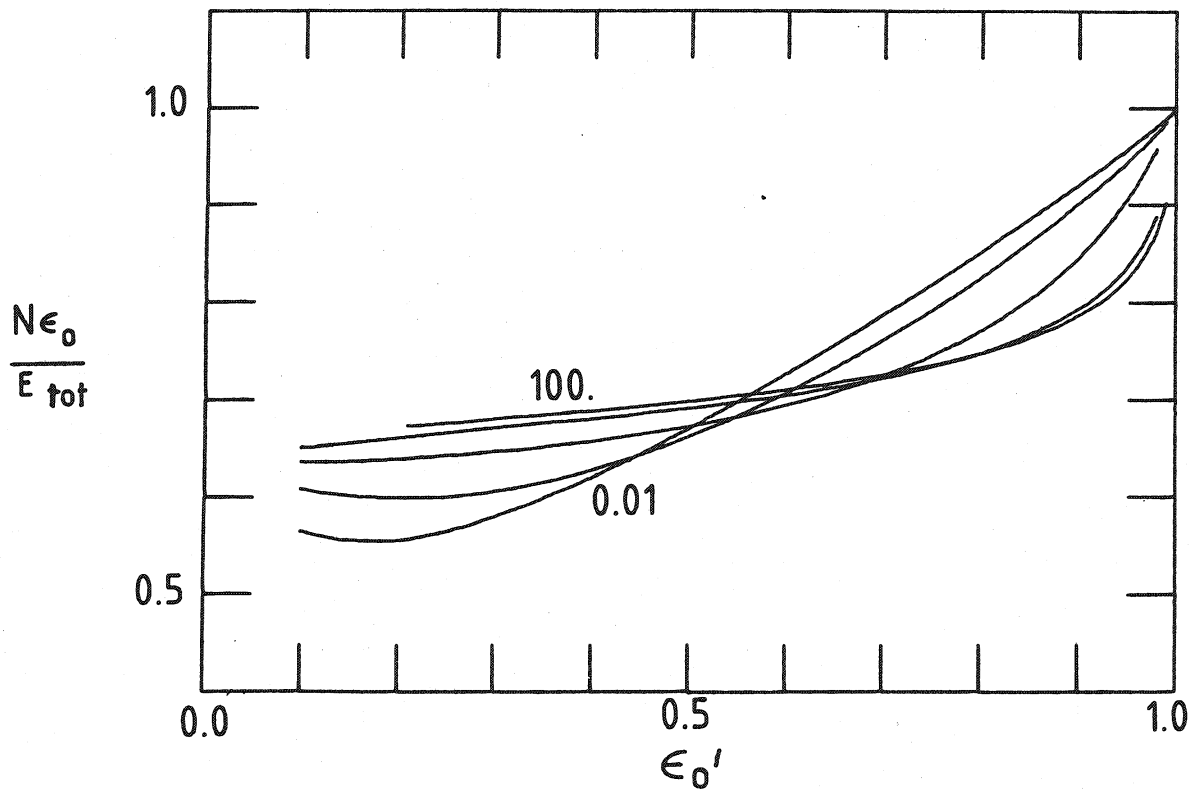


Figure 11

Fig. 12. The dimensionless, scale invariant ratios $E_{\text{tot}} * r_{\text{rms}} / N$ (a), r_{rms} / μ (b) and g_A / g_V (c) given as functions of ϵ' for $s' = 0.01, 0.1, 1.0, 10.0$ and 100.0 . The experimental values for the nucleon ($N=3$) are shown by the dashed lines. The values of g_A / g_V for the nonrelativistic limit (NR), the MIT bag and for the SLAC bag are also indicated in Fig. 12c.

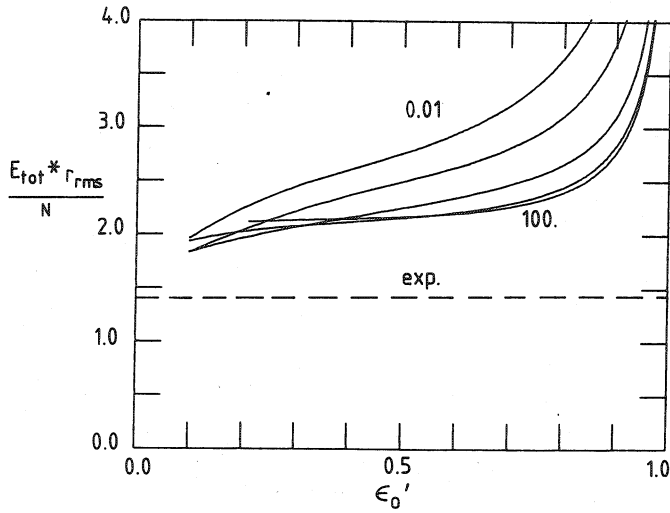


Figure 12a

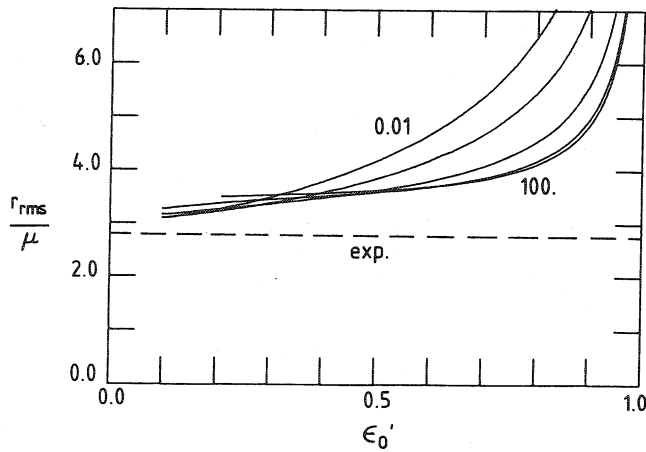


Figure 12b

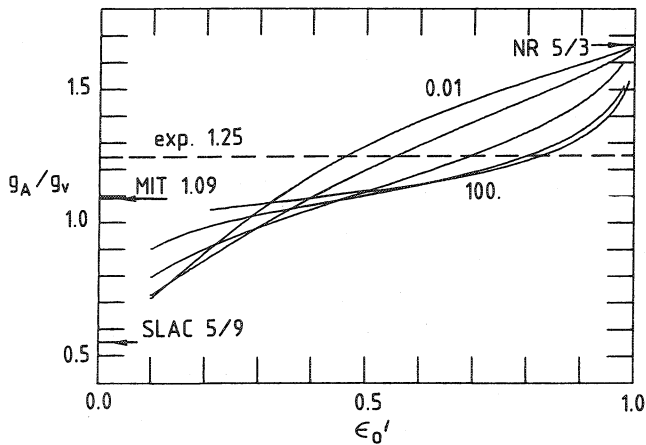


Figure 12c

Fig. 13. At the top are shown the scaled soliton fields when all quarks are in the same $ns_{1/2}$ -state with $n=0, 1$ or 2 nodes of the upper component. At the bottom are shown the corresponding scaled radial functions of the upper $u'(r')$ (solid curves) and lower $v'(r')$ (dashed curves) components as a function of the scaled radius r' . The quark energies are adjusted for $\eta' = Ng^2 = 3000$ and $s' = 0.5$ (see Table III).

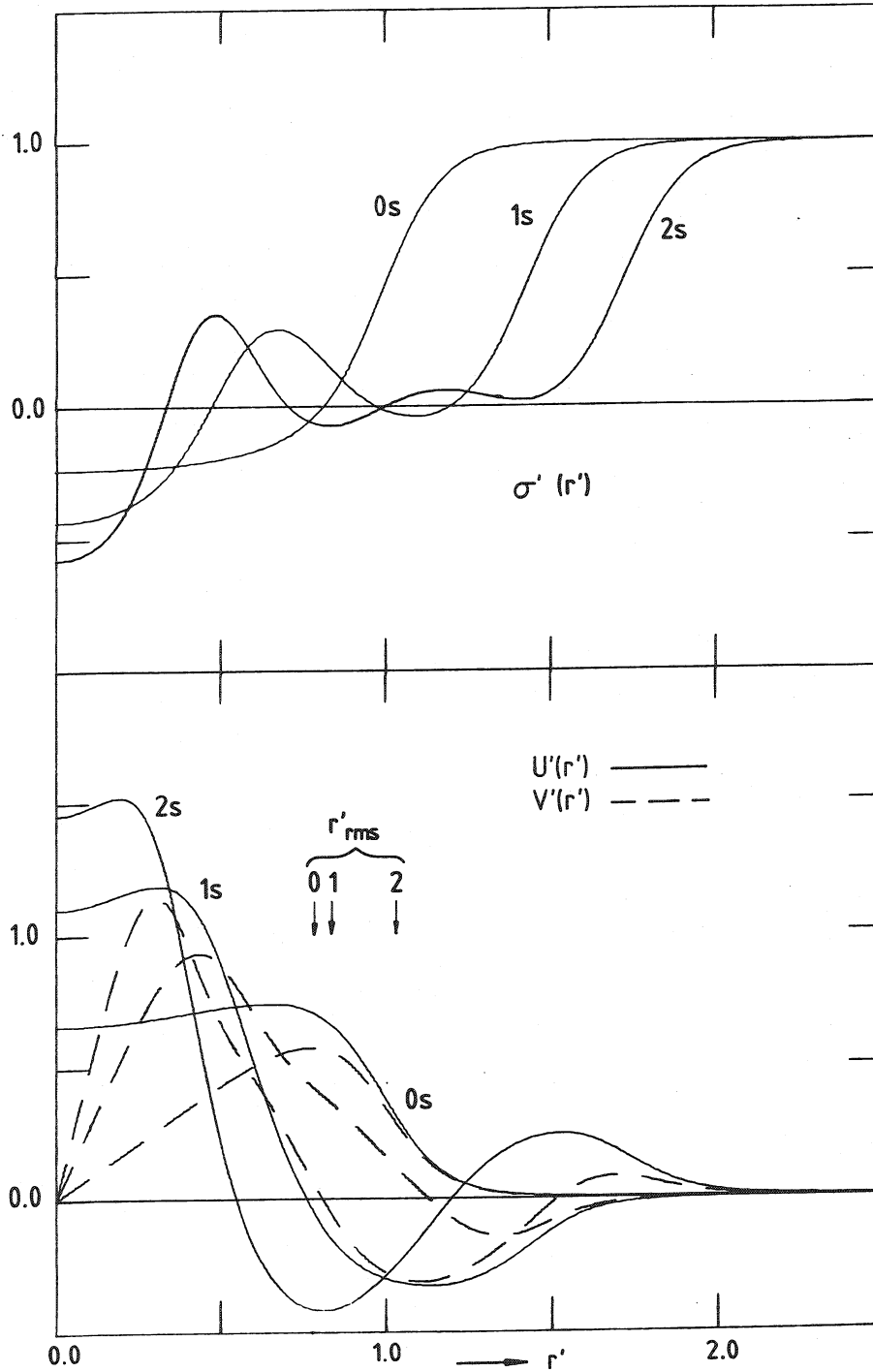


Figure 13

Fig. 14. As in Fig. 13 but when all quarks occupy the same $np_{1/2}$ -state with $n=0, 1$ or 2 nodes of the upper component.

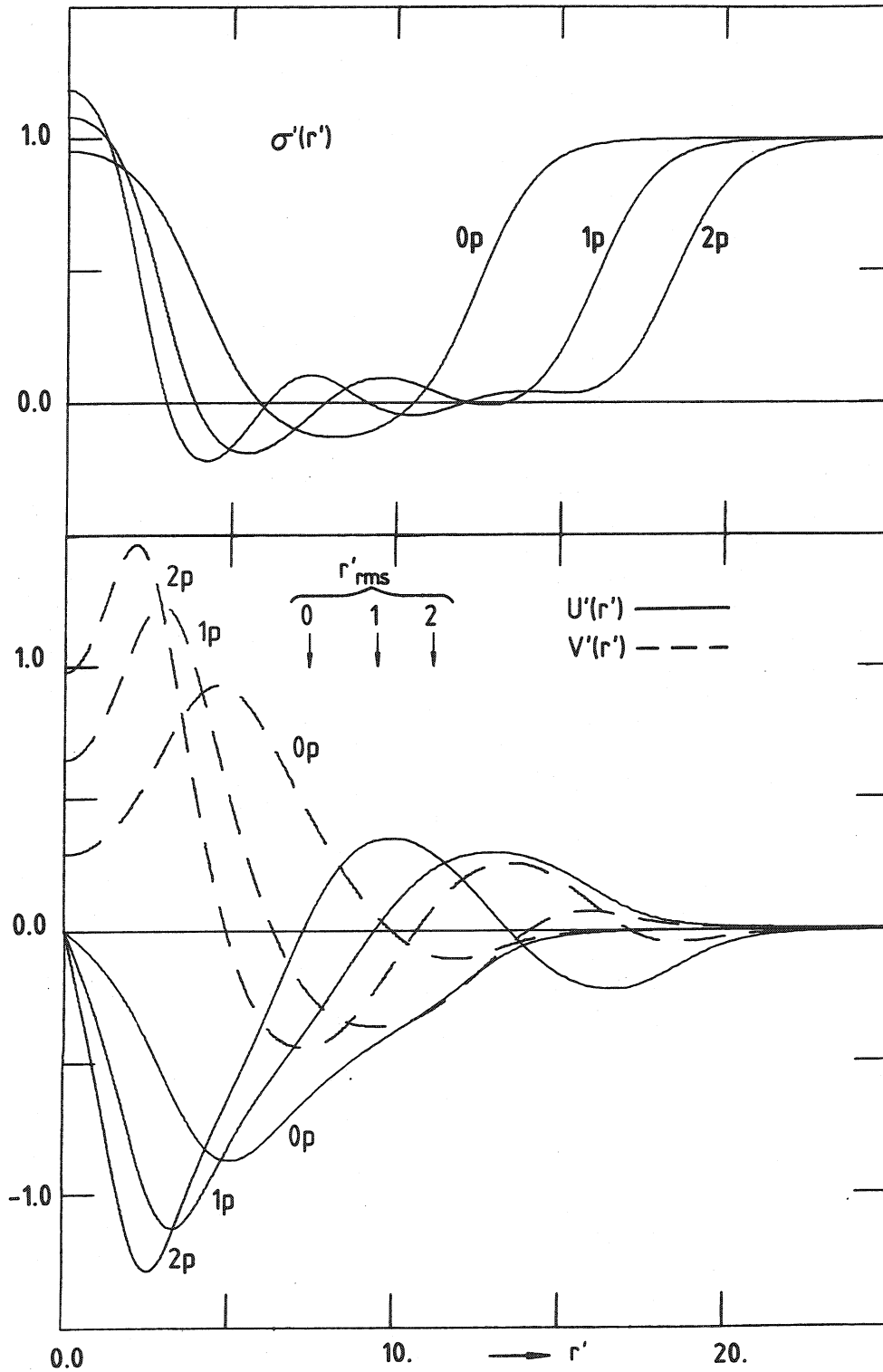


Figure 14

Fig. 15. Solutions for σ' , u'_1 and u'_2 (solid curves) and v'_1 and v'_2 (dashed curves) where 2 quarks are assumed to occupy the ground state $0s_{1/2}$ state (u'_1, v'_1) and 1 quark the 0-node $p_{1/2}$ -wave state (u'_2, v'_2). $g^2 = 1000$ and $s' = 0.5$. (compare Table IV).

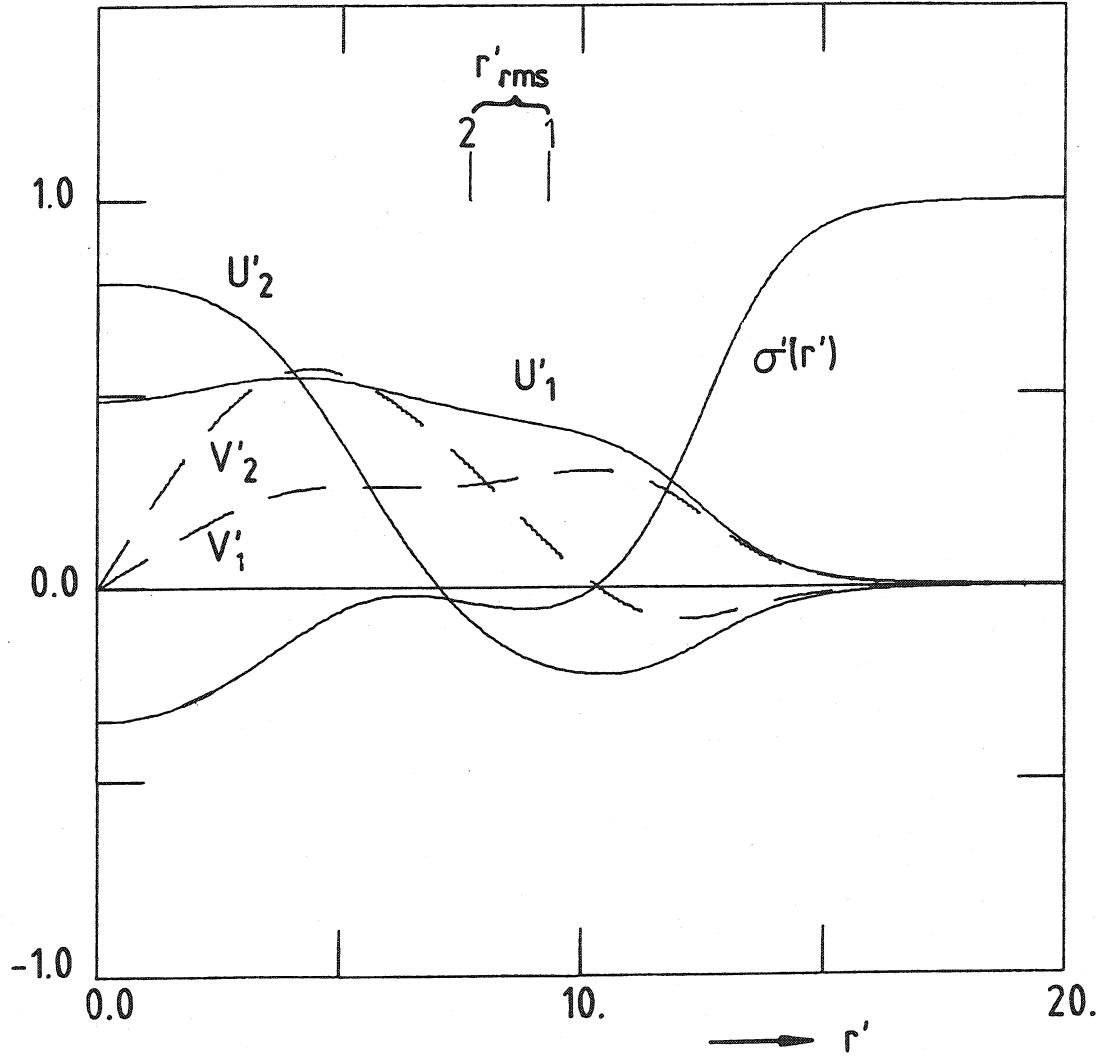


Figure 15

Fig. 16. As in Fig. 15 but where (u'_2, v'_2) is the 1-node $s_{1/2}$ -wave state.

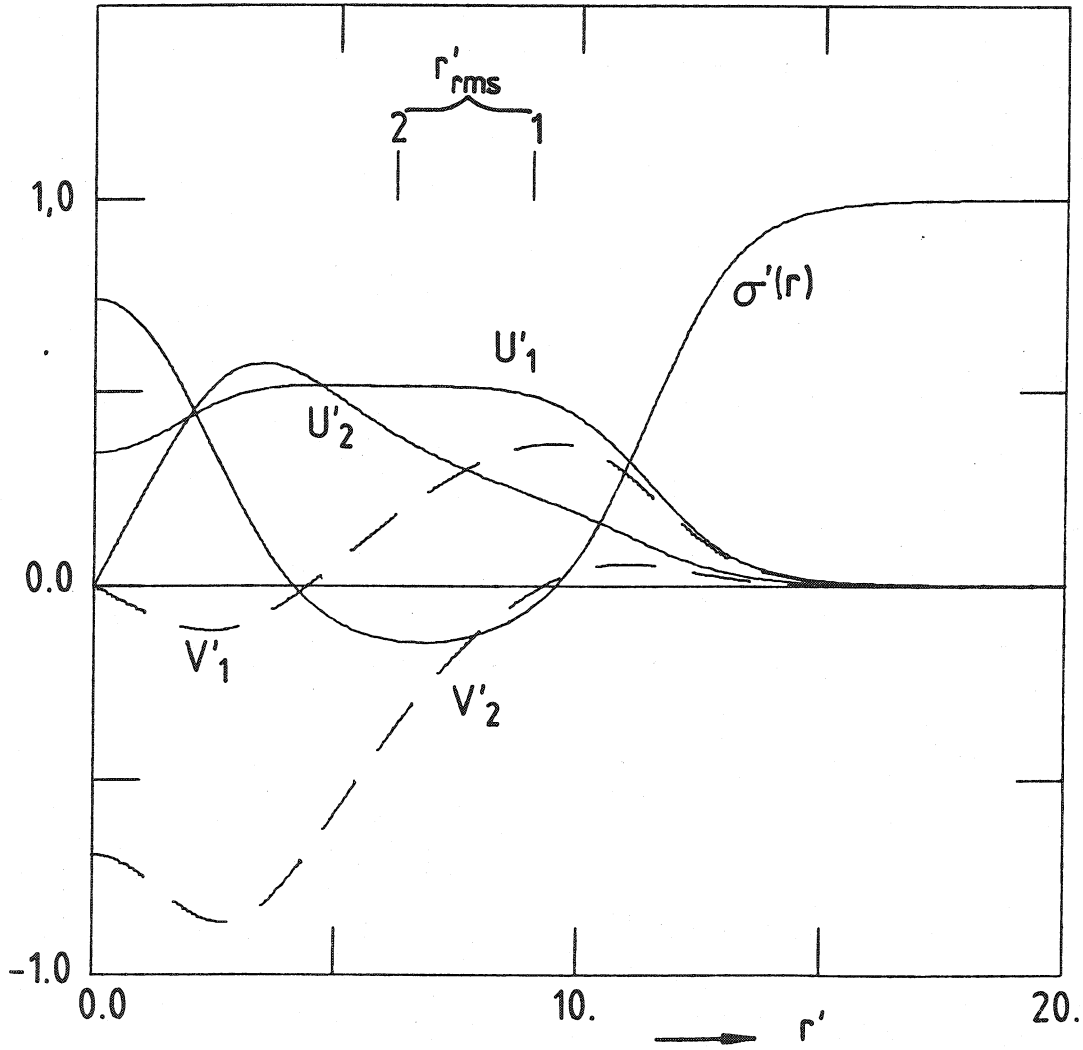


Figure 16

ISSN 0067-0367

To identify individual documents in the series we have assigned an AECL- number to each.

Please refer to the AECL- number when requesting additional copies of this document

from

Scientific Document Distribution Office
Atomic Energy of Canada Limited
Chalk River, Ontario, Canada
K0J 1J0

Price \$4.00 per copy

ISSN 0067-0367

Pour identifier les rapports individuels faisant partie de cette série nous avons assigné un numéro AECL- à chacun.

Veillez faire mention du numéro AECL- si vous demandez d'autres exemplaires de ce rapport

au

Service de Distribution des Documents Office
L'Énergie Atomique du Canada Limitée
Chalk River, Ontario, Canada
K0J 1J0

Prix \$4.00 par exemplaire

©ATOMIC ENERGY OF CANADA LIMITED, 1984

2020-84